Phytomedicine 148 (2025) 157244

Contents lists available at ScienceDirect

Phytomedicine

journal homepage: www.elsevier.com/locate/phymed

Original Article

Salviae Miltiorrhizae Radix et Rhizoma protects against doxorubicin-induced cardiotoxicity: A systematic review

Mei-Yan Yue [a,1], Wai-Rong Zhao [a,1], Shan-Shan Wang [b], Jing Zhang [a], Wen-Ting Shi [a], Jing-Yi Tang [a,**], Zhong-Yan Zhou [a,c,d,*]

[a] Longhua Hospital, Shanghai University of Traditional Chinese Medicine, Shanghai, China
[b] Department of Urology, Fudan University Shanghai Cancer Centre, Shanghai, China
[c] State Key Laboratory of Pharmaceutical Biotechnology, The University of Hong Kong, Hong Kong SAR
[d] Department of Pharmacology and Pharmacy, The University of Hong Kong, Hong Kong SAR

ARTICLE INFO

Keywords:
Salvia miltiorrhiza
Cancer
Doxorubicin, Cardiotoxicity, Traditional Chinese medicine

ABSTRACT

Background: Doxorubicin (DOX) is an effective first-line chemotherapeutic agent used to treat various kinds of cancers. The most serious side effect of DOX is its irreversible cardiotoxicity. *Salviae Miltiorrhizae* Radix et Rhizoma, which is the dry root of the natural plant *Salvia miltiorrhiza* and is named "Danshen" in Chinese, is a widely used Chinese Materia Medica for the treatment of cardiovascular and cerebrovascular disorders in traditional Chinese medicine.

Objective: This study aims to review the potential protective effect of Danshen against DOX-induced cardiotoxicity (DIC).

Methods: A comprehensive systematic search was performed in various electronic databases, including Web of Science, PubMed and Scopus up to July 2025 according to the PRISMA guideline. Two hundred and sixty studies

Abbreviations: AIF, apoptosis-inducing factor; AMPK, AMP-activated protein kinase; ANT, adenine nucleotide translocase; ASFR, adriamycin semiquinone free radical; ATF-6, activating transcription factor-6; CAT, catalase; CDDP, Compound Danshen Dripping Pill; CHD, coronary heart disease; CHF-HKYD, chronic heart failure with heart-kidney yang deficiency; CFDA, China Food and Drug Administration; CK-MB, creatine kinase-MB; COL1A1, homolog family member collagen I A1; CPM, Chinese patent medicine; CPT, cryptotanshinone; CypD, cyclophilin D; DAXX, death-domain-associated protein; DB, Diethyl Blechnic; DIC, DOX-induced cardiotoxicity; DHT, Dihydrotanshinone I; DOX, Doxorubicin; DSS, Danshensu; EF, ejection fraction; ERK, extracellular signal-regulated kinase; ERS, endoplasmic reticulum stress; ESZWD, Ershen Zhenwu Decoction; ETC, electron transport chain; FA, Ferulic acid; FDA, Food and Drug Administration; FS, fractional shortening; FPN, Ferroportin; FTH1, Ferritin Heavy Chain 1; FTMT, Ferritin Mitochondrial; GCLC, glutamate-cysteine ligase catalytic subunit; GPX4, Glutathione Peroxidase 4; GSH, glutathione; GSH-Px, glutathione peroxidase; GSK-3β, glycogen synthase kinase-3β; HO-1, heme oxygenase; IARC, International Agency for Research on Cancer; ICR, Institute of Cancer Research; IKK, IκB kinase; IRE1, inositol-requiring enzyme 1; JNK, c-Jun N-terminal kinase; Keap1, Kelch-like ECH-associated protein 1; LAMP1, Lysosomal-associated membrane protein 1; LDH, lactate dehydrogenase; LV, left ventricular; LVEF, left ventricular ejection fraction; LVFS, left ventricular fractional shortening; LVID, left ventricular internal dimension; MAPKs, mitogen-activated protein kinases; MDA, malondialdehyde; miRNAs, MicroRNAs; MEK, mitogen-activated protein kinase; MMP, mitochondrial membrane potential; mPTP, mitochondrial permeability transition pore; mTORC1, mechanistic target of rapamycin complex 1; NF-κB, nuclear factor kappa B; NQO1, NAD(P)H quinone oxidoreductase 1; Nrf2, nuclear factor erythroid 2-related factor 2; NRF-1, Nuclear respiratory factor 1; ORAC, Oxygen radicals' absorbance capacities; PARP, poly (ADP-ribose) polymerase; PCI, post-percutaneous coronary intervention; PERK, PKR-like ER kinase; PGC-1α, Peroxisome proliferator-activated receptor-γ coactivator 1-α; PRISMA, Preferred Reporting Items for Systematic Reviews and Meta-Analyses; PVT1, plasmacytoma variant translocation 1; QL, Qiliqiangxin; QSG, Qishen Granules; RCTs, randomized controlled trials; RhoA, ras homolog family member A; ROS, reactive oxygen species; ROCK, Rho-associated coiled-coil kinases; *S. miltiorrhiza*, *Salvia miltiorrhiza*; SA, Salvianolic acids; SMAE, *Salvia.miltiorrhiza* aqueous extract; Sal A, Salvianolic acid A; Sal B, Salvianolic acid B; Sal C, Salvianolic acid C; SD, Sprague-Dawley; SERCA, ER Ca^{2+}-ATPase; SIRT3, sirtuin 3; SOD, superoxide dismutase; STS, Sodium tanshinone IIA sulfonate; SYRCLE, Systematic Review Centre for Laboratory animal Experimentation; Tan I, tanshinone I; Tan IIA, tanshinone IIA; TCM, traditional Chinese medicine; TFEB, transcription factor EB; TGF-β, transforming growth factor-beta; TFAM, Mitochondrial Transcription Factor A; TRPC, transient receptor potential canonical; ULK1, unc-51-like autophagy-activating kinase 1; UPR, unfolded protein response; 3-NT, 3-nitrotyrosine.

* Corresponding author at: Department of Pharmacology and Pharmacy & State Key Laboratory of Pharmaceutical Biotechnology, 2/F Laboratory Building, The University of Hong Kong, 21 Sassoon Road, Pokfulam, Hong Kong SAR, China.

** Longhua Hospital, Shanghai University of Traditional Chinese Medicine, Shanghai, China.

E-mail addresses: yuemiyan@126.com (M.-Y. Yue), witoy17@163.com (W.-R. Zhao), wangshanshan_027@163.com (S.-S. Wang), 601729768@qq.com (J. Zhang), 348572363@qq.com (W.-T. Shi), dr_tang@163.com (J.-Y. Tang), biozzy@126.com (Z.-Y. Zhou).

[1] These authors contributed equally to this work.

https://doi.org/10.1016/j.phymed.2025.157244
Received 3 June 2025; Received in revised form 5 August 2025; Accepted 7 September 2025
Available online 8 September 2025

were screened in accordance with a predefined set of inclusion and exclusion criteria. Thirty-five eligible articles were finally included in the current systematic review. All the characteristics and underlying mechanisms of Danshen protecting against DIC were summarized. Additionally, all the Danshen-related clinical trials evaluating their treatment effects for cardiovascular and cerebrovascular diseases were extracted and summarized from the registration databases of clinical trials.

Results: Danshen ameliorated DOX-caused pathological alterations of cardiac cells/tissue, decrease of surviving cardiomyocytes, body weight, heart weight and the ratio of heart to body weight, and increase of mortality. Eleven active ingredients and derivatives of Danshen including tanshinone IIA, sodium tanshinone IIA sulfonate, tanshinone I, salvianolic acid A, salvianolic acid B, salvianolic acid C, cryptotanshinone, ferulic acid, danshensu, dihydrotanshinone I and diethyl blechnic, were identified with potential protective effects against DIC *in vitro* and *in vivo* as well as the eight extracts and formulas of *S. miltiorrhiza* including salvianolic acids, *S. miltiorrhiza* aqueous extract, Compound DanShen Dripping Pill, Danhong injection, Qiliqiangxin, herbal formula B307, Qishen granule and Ershen Zhenwu Decoction. The underlying mechanisms were associated with the Danshen's multiple pharmacological activities, such as anti-apoptosis, anti-oxidative stress, anti-inflammation, anti-mitochondrial dysfunction, maintenance of intracellular Ca^{2+} homeostasis and regulating autophagy by targeting PI3K/Akt/JNK/GSK-3β/mPTP, MAPKs, Bax/Bcl-xL/Caspases, Keap1-Nrf2/NQO1/GPX4, SIRT3/Ac-SOD2, NF-κB, TGF-β/Smads, RhoA/ROCK, AMPK/PGC-1α/NRF-1/TFAM, miR-30a/Beclin1/LAMP1 signaling pathways. Moreover, Danshen-related clinical trials mainly focused on the treatment of cardiovascular and cerebrovascular diseases without clinical trials specifically for the evaluation of Danshen-related agents for the treatment of DIC.

Conclusion: Danshen significantly alleviates DIC according to the previous experimental studies. But no previous study is implemented under cancer condition. A well-designed clinical study that targets certain cancer is an urgent requirement for the verification of Danshen's clinical efficacy in the future, in particular clarifying without affecting the anti-cancer efficacy of DOX.

Introduction

Cancer is the second leading cause of death after cardiovascular diseases in the world (Siegel et al., 2025), and its incidence and mortality rapidly grow along with the increasing ageing population (Filho et al., 2025). According to the statistic report from International Agency for Research on Cancer (IARC), the global burden of cancer was around 20 million new cases with 9.7 million deaths in the year 2022 (Bray et al., 2024). The conventional modalities for cancer treatment are surgery, chemotherapy and radiotherapy (Abbas and Rehman, 2018). Recently, targeted therapy, immuno-inhibition therapy and immune cell therapy have dramatically improved the outcomes of cancers (Huang and Zhou, 2021; Liu et al., 2022; Taefehshokr et al., 2020), but chemotherapy is still the first-line therapeutic approach (Chabner and Roberts, 2005; Pérez-Herrero and Fernández-Medarde, 2015). Although chemotherapy is effectively used for the treatment of numerous types of cancers, it suffers from several restrictions, such as non-specificity and various adverse effects on normal cells and tissues. Hence, its clinical utility is limited due to its side effects (Carvalho et al., 2009; Chabner and Roberts, 2005; Di Nardo et al., 2022; Pabla and Dong, 2012; Zraik and Heß-Busch, 2021), in particular the dose- and time-accumulated cardiotoxicity occurring during the cancer treatment. A related emerging research field named "Onco-cardiology" or "Cardio-oncology" comes into our view.

Doxorubicin (DOX) is an effective chemotherapy drug that belongs to the non-selective class I anthracycline family (Carvalho et al., 2009; Kciuk et al., 2023), which is a first-line chemotherapeutic agent widely used to treat various kinds of cancers, for instance, leukemia, soft tissue sarcomas and breast cancer (Carvalho et al., 2009). However, cardiotoxicity is the most serious side effect caused by the accumulation of DOX treatment (Carvalho et al., 2009; Chotenimitkhun et al., 2015). DOX-induced cardiotoxicity (DIC) is manifested by cardiomyopathy, left ventricular (LV) dysfunction, arrhythmia and congestive heart failure (Mitry and Edwards, 2016). Currently, the treatment strategies, which include the Food and Drug Administration (FDA) approved preventive drug dexrazoxane and conventional cardiovascular drugs, have only achieved modest therapeutic efficacy (Huang et al., 2021a; Octavia et al., 2012; Renu et al., 2018). Understanding the pleiotropic pathological mechanisms of DIC and its timely identification and prevention can reduce the occurrence of cardiovascular complications. There is an urgent need to identify the complex underlying pathological mechanisms of DIC and the novel therapeutic agents, consequently improving the therapeutic achievement of cancer.

Natural products and traditional medicine are precious libraries for human struggling with diseases (Yu et al., 2018b). *Salviae Miltiorrhizae* Radix et Rhizoma, which is the dry root of the natural plant *Salvia miltiorrhiza* (Committee, 2020) and is named Danshen in Chinese, has been a widely used Chinese Materia Medica for the treatment of cardiovascular and cerebrovascular disorders, including atherosclerosis, coronary artery disease and stroke, for thousands of years in Asia (Ji et al., 2000; Zhou et al., 2012). Several Danshen-derived or -contained drugs have been approved by the China Food and Drug Administration (CFDA) and are commercially available in China (Zhou et al., 2019). Danshen presents a high level of safety and effectiveness for the management of human health. However, whether Danshen is effective for the treatment of DIC is controversial currently. In this study, we systematically summarized the protective effects, active ingredients, formulas and underlying mechanisms of Danshen against DIC according to the previous experimental and clinical studies.

Methods

The study protocol of this systematic review was prospectively registered on PROSPERO (CRD420251089204) and the review process followed the PRISMA 2020 guidelines (Page et al., 2021). The PRISMA flow diagram is provided in Fig. 1. Two independent researchers participated in every stage of this study, including article search and selection, data extraction and risk of bias assessment.

Search strategy

We performed a comprehensive systematic search to obtain all relevant studies about "the effect of Danshen on doxorubicin-induced cardiotoxicity" in the electronic databases of PubMed, Scopus and Web of Science up to July 2025. The following diseases and treatments were identified using a combination of Medical Subject Headings (MeSH) and free text terms:

i) "Doxorubicin" OR "Adriamycin" AND
ii) "Danshen" OR "*Salvia miltiorrhiza*" OR "*S. miltiorrhiza*" OR "*Salviae miltiorrhiza* Radix et Rhizoma" OR "Tanshinone IIA" OR "Tanshinone IIA sodium sulfonate" OR "Tanshinone I" OR "Salvianolic acid" OR "Cryptotanshinone" OR "Ferulic acid" OR "Danshensu" OR "Tanshinones" AND

iii) "Heart" OR "Cardiac" OR "Cardiac Toxicity" OR "Cardiomyopathy" OR "Arrhythmias" OR "Myocardium" OR "Myocardial" OR "Myocyte" OR "Cardiomyocyte" OR "Cardiopathic" OR "Cardiopathy" OR "Cardiotoxicity" OR "Cardiotoxicities" OR "Cardiac Fibrosis" OR "Cardiac Inflammation" in title, abstract or keywords.

Inclusion and exclusion criteria

The inclusion criteria were considered: (1) Clinical, *in vivo* and *in vitro* studies without restriction on publication year; (2) Studies focusing on the role of *S. miltiorrhiza* in DIC; (3) Independent, full-text scientific studies with original data.

The exclusion criteria comprised: (1) Studies examining active ingredients derived from non-*S. miltiorrhiza* plants; (2) Research on organ toxicity unrelated to cardiotoxicity; (3) Investigations involving drug combinations; (4) Studies lacking a control group; (5) Unrelated articles, review papers, case reports, book chapters, letters to editors, oral presentations, posters and editorials.

Data extraction and management

Each eligible study was evaluated by two independent researchers and the following data were then extracted: (1) author name and year of publication; (2) models (clinical, *in vivo* and/or *in vitro*); (3) dosage, protocol of usage, and administration route of DOX; (4) outcomes of DOX on cardiac cells/tissue injury and heart dysfunction; (5) dosage, experimental protocol, and administration route of Danshen and/or its related extracts, ingredients, derivatives and formulas; (6) administration outcomes.

Methodological quality appraisal for in vivo studies

The methodological quality of *in vivo* studies was assessed by the SYRCLE's risk of bias (RoB) tool (Hooijmans et al., 2014). The resulting RoB tool for animal studies contains 10 entries. These entries are related to 6 types of bias including selection bias, performance bias, detection bias, attrition bias, reporting bias and other biases. Each SYRCLE domain was judged as Low risk (indicating adequate methodological safeguards), High risk (reflecting inadequate methods likely to introduce bias) or Unclear risk (denoting insufficient reporting preventing definitive assessment). The items were judged "Low" risk as 1 point, and both "Unclear" and "High" as 0 points. The total score of the 10 items was considered as the quality score of each study. Two reviewers (M.Y.Y. and W.R.Z.) evaluated each study independently. Disagreements were resolved by consensus or a third reviewer (Z.Y.Z.).

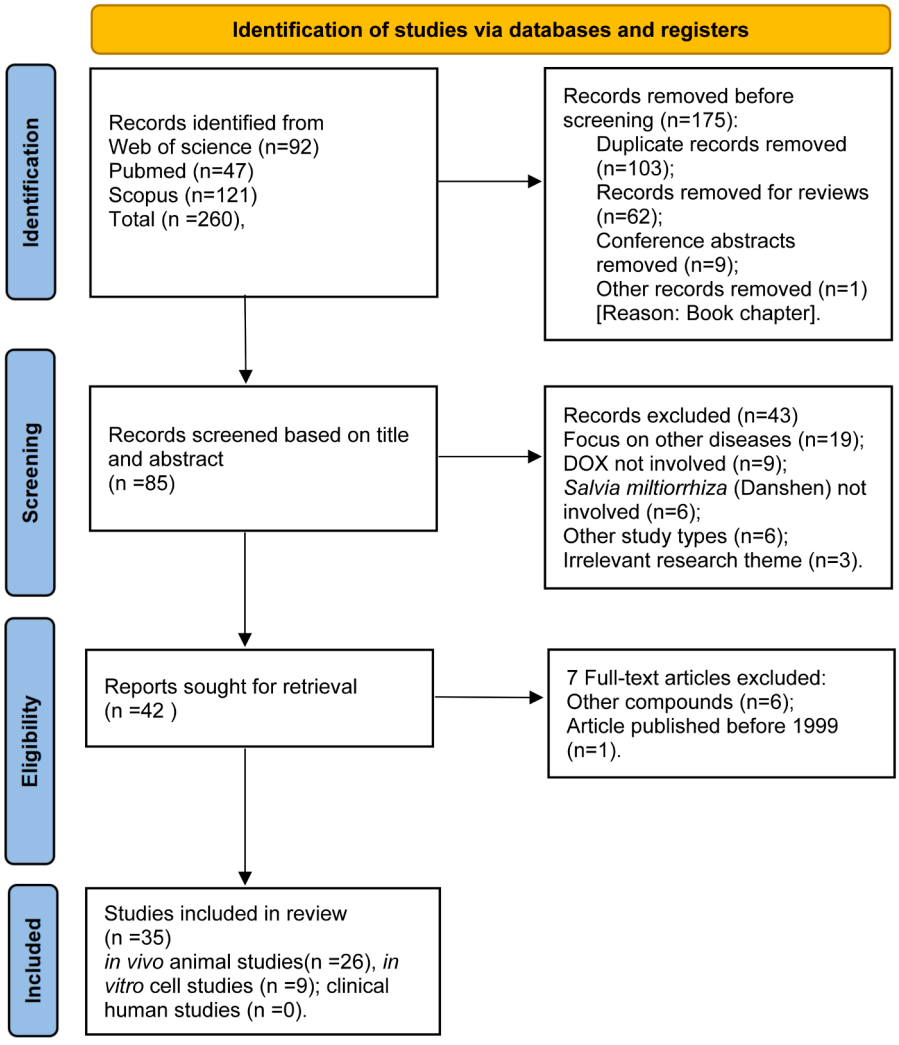

Fig. 1. Schematic diagram of the PRISMA guideline for screening of research articles.

Results

Literature search and screen

Two hundred and sixty articles were obtained by systematically searching the above-mentioned electronic databases up to July 2025. One hundred seventy-five records were removed before screening, which included 103 duplicates, 62 reviews, 9 conference abstracts and 1 book chapter. The remaining 85 records were screened based on titles and abstracts according to the inclusion/exclusion criteria, resulting in 43 exclusions with the reasons including other diseases [n=19], DOX not involved [n=9], *S. miltiorrhiza* not involved [n=6], other study types [n=6] and irrelevant theme [n=3]. Forty-two research articles were qualified for evaluation of their full texts, in which 7 articles were excluded with the reasons of other compounds [n=6] and published before 1999 [n=1]. Finally, thirty-five articles (26 *in vivo* animal studies,9 *in vitro* cell studies and 0 clinical human studies) were included in the current study (Fig. 1), and a comprehensive summary of detailed information of literature search strategy and the related data extracted from the databases is listed in the **Supplemental materials**.

Risk of bias assessment

In this review, the SYRCLE checklist was used to evaluate the risk of bias for the 26 *in vivo* animal studies (Table 1). The quality scores ranged from 1 to 4 points for the sum of parameters in which Selective Outcome Reporting, Baseline Characteristics and Incomplete Outcome Data most frequently showed low risks of bias. Random Housing and Blinding of Caregivers/Investigators were consistently high-risk across all studies. Allocation Concealment and Blinding of Outcome Assessors also frequently showed high risk. Sequence Generation and Random Outcome Assessment were almost unclear.

We used “High” to indicate a high risk of bias, or “Unclear” to indicate an undetermined level of bias due to insufficient data. The items judged as “Low” were scored one point, and the sum scores of 10 items were presented for the quality score of each study. Future studies should pay particular attention to the detailed reporting and implementation of random sequence generation, allocation concealment, random housing procedures, blinding of caregivers/investigators, blinding of outcome assessors and random outcome assessment. Improving these methodological aspects will significantly enhance the reliability and rigor of the research.

Danshen protects against doxorubicin-induced cardiotoxicity

According to the previous phytochemical studies, to date, a variety of chemical constituents of Danshen have been well identified and they are mainly divided into two categories, which include more than 30 lipophilic compounds that have a diterpene quinone structure (tanshinone I–VI, cryptotanshinone, isotanshinone I–II, Danshenol A, etc.) and more than 50 hydrophilic compounds that have a phenolic acid structure (Danshensu, salvianolic acid A, salvianolic acid B, salvianolic acid C, protocatechuic aldehyde, etc.) (Chen et al., 2014; Li et al., 2018b; Wang et al., 2007; Zhou et al., 2005). In addition, nitrogenous compounds, lactones, polysaccharides, flavonoids, steroids, triterpenes and other components were also identified from Danshen. In order to evaluate the potential of Danshen treating DIC, we reviewed all the 35 identified studies involving the protective effects of Danshen against DIC, and systematically summarized the active ingredients and their derivatives, extracts and formulas that contain Danshen in Table 2 as well as their detailed experimental models, dosages, outcomes and underlying mechanisms.

The ingredients of Danshen and their derivatives protect against doxorubicin-induced cardiotoxicity

Eleven compounds, which are isolated from Danshen, and their derivatives are included in the current review and their structures are listed in Fig. 2. They all presented potential protection against DIC with multiple molecular mechanisms according to previous studies.

Diterpenoids

Tanshinone I. Tanshinone I (Tan I, $C_{18}H_{12}O_3$), which belongs to the abietane diterpenoids, is one of the main lipophilic ingredients/tanshinones isolated from *S. miltiorrhiza* (Li et al., 2018a). It presents various pharmacological functions, particularly in cancer (Huang et al., 2021b). Previous experimental studies provided evidence that post-treatment of Tan I significantly increased the left ventricular ejection fraction (LVEF) and left ventricular fractional shortening (LVFS) and decreased the left ventricular internal dimension (LVID) against DOX-induced cardiac dysfunction according to the echocardiography examination in C57BL/6 mice (Jiang et al., 2022a; Jiang et al., 2022b). Tan I also ameliorated the cardiomyoblast H9c2 morphology and inflammatory infiltration in the heart, and decreased the cardiac injury markers creatine kinase-MB (CK-MB) and lactate dehydrogenase (LDH) in serum. In addition, Tan I protected against DIC in rat cardiomyoblast H9c2, and enhanced the anti-cancer effect of DOX in lung cancer cell line A549. Tan I also ameliorated the mitochondrial structural and functional damage in DOX-stressed H9c2 cells (Jiang et al., 2022b). Thus, we could conclude that Tan I potentially protects against cardiac dysfunction and myocardial structural injury in DIC.

Tanshinone IIA. Tanshinone IIA (Tan IIA, $C_{19}H_{18}O_3$) is a lipophilic compound derived from *S. miltiorrhiza* and demonstrates diverse cardiovascular benefits, for instance, vasodilation and cardioprotection (Gao et al., 2008; Hong et al., 2012; Yu et al., 2020). *In vitro* studies demonstrated that Tan IIA significantly enhanced cell viability and mitigated DOX-induced apoptosis in H9c2 rat cardiomyoblast, HL-1 mouse cardiac cells and primary cultured neonatal Sprague-Dawley (SD) rat cardiomyocytes (Gao et al., 2008; Guo et al., 2018; Hong et al., 2012; Song et al., 2017; Wang et al., 2019a; Wang et al., 2019b; Xu et al., 2022a). According to the results from echocardiography, Tan IIA restored DOX-induced cardiac dysfunction and histological analysis demonstrated its prevention of myocardial structural alterations and myofibrillar disruption (Xu et al., 2022a). DOX disrupted autophagosome/autolysosome equilibrium and downregulated autophagic flux in cardiomyoblast H9c2 while Tan IIA rectified autophagic flux and bolstered cell viability by augmenting autophagosome formation and autolysosome degradation (Wang et al., 2019a). In addition, Tan IIA dose-dependently increased the cell viability of both H9c2 and HL-1 cells, ameliorated cell morphology change, and reduced intracellular reactive oxygen species (ROS) generation (Guo et al., 2018; Song et al., 2017; Wang et al., 2019a; Xu et al., 2022a). In neonatal rat cardiomyocytes, Tan IIA shielded against DOX-induced cell apoptosis by diminishing TUNEL-positive apoptotic cells, decreasing caspase-3 activity, inhibiting cytochrome c translocation from mitochondria to cytosol, upregulating the anti-apoptotic protein Bcl-xL, and reducing apoptotic nuclear morphology and hypo-diploid cell population (Gao et al., 2008; Hong et al., 2012). In both zebrafish and C57BL/6 mice

Table 1
The bias risk assessment of *in vivo* studies.

Study ID	Selection bias			Performance bias		Detection bias		Attrition bias	Reporting bias	Other bias	Quality score
	Sequence generation	Baseline characteristics	Allocation concealment	Random housing	Blinding	Random outcome assessment	Blinding	Incomplete outcome data	Selective outcome Reporting	Other sources of bias	
Linhao Xu et al. & 2022 (Xu et al., 2022a)	Unclear	Unclear	High	High	High	Unclear	High	Unclear	Low	Unclear	1
Xiaoping Wang et al. & 2019 (Wang et al., 2019a)	Unclear	Low	Unclear	High	High	High	High	Low	Low	Low	4
Zhaohui Guo et al. & 2018 (Guo et al., 2018)	Unclear	Low	Unclear	High	High	High	High	Low	Low	Low	4
Baohong Jiang et al. & 2009 (Jiang et al., 2009)	Unclear	Unclear	High	High	High	Unclear	High	Unclear	Low	Unclear	1
Guangyin Zhou et al. & 2002 (Zhou et al., 2002)	Unclear	Low	Unclear	High	High	High	High	Low	Low	Low	4
Guangyin Zhou et al. & 1999 (Zhou et al., 1999)	Unclear	Low	Unclear	High	High	High	High	Low	Low	Low	4
Qianqian Jiang et al. & 2022 (Jiang et al., 2022b)	Unclear	Unclear	Unclear	Unclear	Unclear	Unclear	Low	Unclear	Unclear	Unclear	1
Qianqian Jiang et al. & 2022 (Jiang et al., 2022a)	Unclear	Unclear	High	High	High	Unclear	Unclear	Unclear	Low	Unclear	1
Rongchang Chen et al. & 2017 (Chen et al., 2017)	Unclear	Unclear	Unclear	Unclear	Unclear	Unclear	Low	Unclear	Unclear	Low	2
Rongchang Chen et al. & 2016 (Chen et al., 2016)	Unclear	Unclear	Unclear	Unclear	Unclear	Unclear	Low	Unclear	Unclear	Unclear	1
Le Li et al. & 2020 (Li et al., 2020)	Unclear	Unclear	High	High	High	Unclear	High	Unclear	Low	Unclear	1
Yanshan Zhang et al. & 2016 (Zhang et al., 2016b)	Unclear	Unclear	High	High	High	Unclear	High	Unclear	Low	Unclear	1
Urmila Aswar et al. & 2019 (Aswar et al., 2019)	Unclear	Low	Unclear	High	High	High	High	Low	Low	Low	4
Jiaying Qi et al. & 2022 (Qi et al., 2022)	Unclear	Low	Unclear	High	High	High	High	Low	Low	Low	4
Xiaojiao Yi et al. & 2022 (Yi et al., 2022)	Unclear	Low	Unclear	Unclear	Unclear	Unclear	Unclear	Low	Low	Low	4
Xiaoping Wang et al. & 2020 (Wang et al., 2020a)	Unclear	Low	High	High	High	Unclear	Unclear	Low	Low	Low	4
Ke Feng et al. & 2021 (	Unclear	Unclear	High	High	High	Unclear	High	Unclear	Low	Unclear	1

(*continued on next page*)

Table 1 (*continued*)

Study ID	Selection bias			Performance bias		Detection bias		Attrition bias	Reporting bias	Other bias	Quality score
	Sequence generation	Baseline characteristics	Allocation concealment	Random housing	Blinding	Random outcome assessment	Blinding	Incomplete outcome data	Selective outcome Reporting	Other sources of bias	
Feng et al., 2021)											
Jianxuan Li et al. & 2024 (Li et al., 2024a)	Unclear	Low	Unclear	High	High	High	High	Low	Low	Low	4
Baohong Jiang et al. & 2008 (Jiang et al., 2008)	Unclear	Unclear	Unclear	Unclear	Unclear	Unclear	Unclear	Unclear	Unclear	Low	1
YuChiang Hung et al. & 2020 (Hung et al., 2020)	Unclear	Low	Unclear	Unclear	Unclear	Unclear	Unclear	Low	Low	Low	4
JyhSheng You et al. & 2007 (You et al., 2007)	Unclear	Low	Unclear	High	High	High	High	Low	Low	Low	4
Xutao Sun et al. & 2020 (Sun et al., 2020)	Unclear	Low	Unclear	High	High	High	High	Low	Low	Low	4
ChiaYing Lien et al. & 2015 (Lien et al., 2015)	Unclear	Low	Unclear	High	High	High	High	Low	Low	Low	4
Jingmei Zhang et al. & 2024 (Zhang et al., 2024)	Unclear	Low	Unclear	High	High	High	High	Low	Low	Low	4
Siming Xue et al. & 2024 (Xue et al., 2024)	Unclear	Low	Unclear	High	High	High	High	Low	Low	Low	4
Dan Cheng et al. & 2025 (Cheng et al., 2025)	Unclear	Unclear	High	High	High	Unclear	High	Unclear	Low	Unclear	1

The items judged as "Low" were scored 1 point, and both "High" and "Unclear" were scored as 0 point. The sum scores of the 10 items were presented as the quality score of each study.

models of DIC, Tan IIA improved cardiac performance and reversed structural abnormalities, such as myocardial cell structure disorder, myofibril loss, karyopyknosis and plasma dissolving myocardial cells (Wang et al., 2019a). In the mouse DIC model, Tan IIA markedly enhanced cardiac function by suppressing apoptosis and reinstating autophagy (Wang et al., 2019a; Xu et al., 2022a). Pretreatment of Tan IIA attenuated DOX-induced myocardial injury by improvement of histopathology, reduction of serum myocardial enzyme levels and enhancement of antioxidant enzyme activities in both C57BL/6 and SD mice (Gao et al., 2008; Wang et al., 2019a; Xu et al., 2022a). These findings demonstrate that Tan IIA exerts comprehensive cardioprotective effects against DIC via multiple mechanisms, including anti-apoptotic activity, autophagy regulation and antioxidant pathways.

Cryptotanshinone. Cryptotanshinone (CPT, $C_{19}H_{20}O_3$), a diterpenoid quinone, is one of the major lipophilic constituents extracted from *S. miltiorrhiza* (Han et al., 2008). CPT mitigated DOX-induced cell damage by attenuating apoptosis, reducing ROS production and preserving mitochondrial membrane potential in rat cardiomyoblast H9c2 (Li et al., 2020; Wang et al., 2021a). Oral administration of CPT alleviated DOX-induced declines of cardiac function and histopathological alterations, including cardiac fibrosis and cardiomyocyte apoptosis, in Wistar rats (Li et al., 2020). CPT bolstered the antioxidant capacity of cardiomyocytes by augmenting superoxide dismutase (SOD), catalase (CAT) and glutathione peroxidase (GSH-Px) activities while reducing the level of the lipid peroxidation product malondialdehyde (MDA) in both Wistar rat hearts and H9c2 cells. The antioxidant activity of CPT diminished DOX-induced ROS generation and attenuated oxidative stress, thereby protecting cardiomyoblast H9c2 from DOX-induced cell death (Jiang et al., 2022b; Li et al., 2020; Zhang et al., 2016b).

Dihydrotanshinone I. Dihydrotanshinone I (DHT, $C_{18}H_{14}O_3$) is one of the major lipophilic diterpenes isolated from *S. miltiorrhiza* (Gao et al., 2017). DHT effectively prevents DOX-induced inflammation, apoptosis and oxidative stress in rat cardiomyoblast H9c2 and mouse macrophages RAW264.7 (Wang et al., 2020b; Yu and Qian, 2020; Yuan et al., 2019b). Macrophage recruitment is crucial for cardiac tissue homeostasis (Ma et al., 2018). DHT suppressed M1 macrophage activation and excessive release of pro-inflammatory cytokines, such as TNF-α and IL-8, in H9c2 cells, RAW264.7 cells, zebrafish and C57BL/6 mice (Wang et al., 2020a). H&E staining results revealed that DHT treatment prevented inflammatory cell infiltration and cellular injury in heart, along with decreasing oxidative stress markers ROS and MDA (Wang et al., 2020a).

The protective effects of DHT were validated in both zebrafish and C57BL/6 mouse models of DIC with significantly improved cardiac function and mitigated structural damage (Wang et al., 2020a). In the zebrafish model, two days exposure of DOX-induced multiple cardiac abnormalities including pericardial edema and tail blood accumulation

Table 2
The comprehensive evaluation of Danshen-associated drugs, including the active ingredients and their derivatives, extracts and formulas, protecting against DIC.

Active component	Model	DOX dosage & protocol of usage; administration route	Detection methods & technology	Outcomes of DOX on cardiac cells/ tissue	Danshen dosage & protocol of usage; administration route	Danshen coadministration outcomes	Author & year
Tanshinone IIA (Tan IIA)	Male C57BL/6 mice (7 weeks old, 20 g); H9c2 cells; HL-1 cells	C57BL/6 mice: 3 mg/kg every 3 days *i.p.* & 21 days; H9c2 and HL-1 cells: DOX 60 μM & 24 h	MTT, Hoechst 33342, TUNEL, RNA-seq, bioinformatics analysis, TRIzol Reagent, qRT-PCR, Echocardiographic, H&E, TUNEL, TEM, Western blot	Apoptosis↑, cell viability↓, caspase-3↑, caspase-8↑, DAXX↓, p-ERK1/2↓, p-MEK↓, p-P38↑, MDR1 mRNA↑, MRP1 mRNA↑, LVEF↓, LVFS↓, LVIDs↑,myocardial structural damage, myofibril disruptio, cardiac function↓	C57BL/6 mice: DOX 3 mg /kg every 3 days *i.p.* & 21 days + Tan IIA 2.5, 5 and 10 mg/kg/day *i.p.* & 28 days (7 days of pretreatment before DOX); DOX every 3 days *i.p.* & 21 days + NAC 200 mg/kg *i.p.* & 28 days; H9c2 and HL-1 cells: DOX 60 μM + 10, 20 and 40 μM Tan IIA & 24 h	Activating the DAXX/MEK/ERK1/2 pathway, MDR1↓, MRP1↓, DAXX↑, p-ERK1/2↑, p-MEK↑, caspase-8↓, p-P38↓, MDR1 mRNA↓, MRP1 mRNA↓ caspase-3↓, LVEF↑, LVFS↑, LVIDs↓, cardiac function↑, reduced myocardial damage	Linhao Xu et al. & 2022 (Xu et al., 2022a)
	Zebrafish; C57BL/6 mice (20 g ± 2 g); H9c2 cells	Zebrafish: 100 μM DOX & 3 dpf; C57BL/6 mice: DOX 5mg/kg *i.p.* once per week & 4weeks; H9c2 cells: DOX 1 μM & 24 h	Echocardiographs, H&E, TUNEL, TEM, Western blot, CCK-8, GFP-mRFP-LC3 adenovirus transfection, Cathepsin B activity assay, GFP-TFEB lentiviral transfection.	Autolysosome↑, Bcl-2↓, Bax↑, LC3-II↑, P62↑, Beclin1↓, LAMP1↓, Cathepsin B activity↓, mTOR activation↑, EF↓, FS↓, LVEDD↑, LVESD↑, LDH↑, CKMB↑, cardiotoxicity↑	Zebrafish: 100 μM DOX and 20 μM Tan IIA & 3 dpf; C57BL/6 mice: DOX 5 mg/kg *i.v.* once per week & 4 weeks + Tan IIA 10 mg/kg *i.g.*; H9c2 cells: DOX 1 μM + Tan IIA 1 μM & 24h	Heart function↑, reversed pathological, autophagosome↑, Bcl-2↑, Bax↓, LC3-II↓, P62↓, Beclin1↑, LAMP1↑, Cathepsin B activity↑, mTOR activation↓, EF↑, FS↑, LVEDD↓, LVESD↓, LDH↓, CKMB↓, proliferative activity↓	Xiaoping Wang et al. & 2019 (Wang et al., 2019a)
	H9c2 cells	DOX 5 μmol /L & 48h	CCK-8, immunofluorescence staining, LDH assay, western blot	Cells viability↓, LDH↑, autophagy degree↑, AMPK activation↓	DOX 5 μmol /L + Tan IIA 10 mg /L & 48h	Cells viability↑, LDH↓, autophagy degree↑, AMPK activation↑	Zhaohua Wang et al. & 2019 (Wang et al., 2019b)
	Male Institute of Cancer Research mice (25-29 g); H9c2 cells	ICR mice: DOX 18 mg/kg *i.p.* on day 5; H9c2 cells: DOX 1 μM & 24 h	H&E, MTT, fluorospectrophotometer analysis, RT-qPCR, western blot, siRNA transfection	Myocardial injury↑, myocardial fiber fragmentation and gap enlargement ↑, Serum myocardial enzymes AST↑, LDH↑, CK↑ CK-MB↑, SOD↓, CAT↓, GSH ↓, MDA↑, NQO1↑, MRP2↑, P-gp↑, ROS↑, GSH↓	ICR mice: DOX 18 mg/kg *i.p.* & day 5 + Tan IIA (15 and 30 mg/kg) *i.p.* & 7 days (pretreatment 4 days before DOX, then 2 days after); H9c2 cells: DOX 1 μM & 24 h + Tan IIA 1, 3, 5, 10 μM, pretreatment for 4 h before 1 μM DOX & 24 h	AST↓, LDH↓, CK, CK-MB activity↓, SOD↑, CAT↑, GSH ↑, MDA ↓, Nrf2↑, HO-1↑, NQO1 ↑, GCLC↑, MRP2↓, P-gp ↓, ROS↓, GSH↑	Zhaohui Guo et al. & 2018 (Guo et al., 2018)
	H9c2 cells	DOX 10 μM & 24h	CCK-8, RT-PCR, Annexin V/PI double staining, luciferase reporter assay, western blot immunoblotting, luciferase reporter assay	Myocardial apoptosis↑, miR-133↓, caspase-9↑	DOX 10 μM + TanIIA 5, 10 μM & 24 h	Myocardial apoptosis↓, miR-133↑, caspase-9↓	Tao Song et al. & 2017 (Song et al., 2017)
	Primary cultured neonatal SD rat cardiomyocytes	DOX 1 μM & 12h and 24h	TUNEL, Caspase-3 activity assay, Western blot, Flow cytometric assay, Short interfering RNA (siRNA) transfection	The percentage of apoptotic cells↑, ROS↑, p-Akt↓, caspase-3 ↑	DOX 1 μM & 0.1, 0.3, 1 and 3 μM Tan IIA & 12 h	The percentage of apoptotic cells↓, ROS ↓, p-Akt ↑, caspase-3↓	HongJye Hong et al. & 2012 (Hong et al., 2012)
	Primary cultured neonatal SD rat cardiomyocytes	DOX 1 μM & 24 h	MTT, Hoechst 33342 staining, DCF fluorescence, DHE fluorescence, western blotting	Bcl-2/Bax↓, apoptosis↑, ROS↑	DOX 1 μM & 24 h + Tan IIA (0.5–2μM) pre-treated & 2 h	Bcl-2/Bax↑, apoptosis↓, ROS↓	Jie Gao et al. & 2008 (Gao et al., 2008)
Sodium tanshinone IIA sulfonate (STS)	Adult male KM mice (21.9±1.1g); H9c2 cells	KM mice: DOX 5 mg/kg *i.p.* & day 1, 8, 15; H9c2 cells: DOX 1 μM & 24 h	CCK-8, Hoechst 33342, ECG, TTR, Histopathologic detection, Fibrillar collagen stain, H&E	Survival rate↓, apoptosis↑, heart rate↓, heart size↓, body weight↓, ST-interval↑ , QRS interval↑ ; HW/TL ratio↓, myocardial TTR↓, myocardial vacuolization/myofibrillar loss, ventricular cavity dilation, perivascular fibrosis↑	KM mice: DOX 5 mg/kg *i.p.* & day 1, 8, 15 + STS 5 mg/kg and 15 mg/kg *i.p.* at 0.5, 24, 48 and 72 h post-modeling; H9c2 cells: DOX 1 μM & 24 h + (0, 1.6, 8, 40) μM STS	Survival rate↑, apoptosis↓, heart rate↑, ventricular cavity dilation↓, myocardial structure↑, ST-interval↓, QRS interval↓, HW/TL ratio↑ , TTR↑, reduced myocardial vacuolization/myofibrillar loss, attenuated ventricular dilation, decreased perivascular fibrosis	Baohong Jiang et al. & 2009 (Jiang et al., 2009)

(*continued on next page*)

Table 2 (*continued*)

Active component	Model	DOX dosage & protocol of usage; administration route	Detection methods & technology	Outcomes of DOX on cardiac cells/ tissue	Danshen dosage & protocol of usage; administration route	Danshen coadministration outcomes	Author & year
	Adult male SD rats (180-200 g)	DOX 4 mg/kg *i.v.* weekly & 4 weeks	Electron Spin Resonance, Thiobarbituric Acid Reactive Substrates (TBARS) assay, spectrophotometric method	Lipid peroxidation↑,rapid generation of adriamycin semiquinone free radical, ASFR oxidation to O_2^{-}/·OH (DMPO-OH signal), TBARS↑, mitochondrial swelling↑	DOX 4 mg/kg, *i.v.* + STS 30 mg/kg, *i.p.* weekly & 4 weeks	delay of ASFR appearance, lipid free radicals↓, lipid peroxidation↓, 4-POBN signal↓, TBARS↑, mitochondrial swelling↓	Guangyin Zhou et al. & 2002 (Zhou et al., 2002)
	Male BALB c mice (20±2g)	DOX 4mg/kg *i.v.* weekly & 4 weeks	Buege, Aust, autooxidation of pyrogallol, DTNB method, spectrophotometric method, ESR	Myocardial lipid peroxidation↑, mitochondrial lipid peroxidation and swelling↑, ROS↑	DOX 4 mg/kg *i.v.* + STS 30 mg /kg *i.p.* 30 min before DOX *i.v.* weekly & 4 weeks	Myocardial lipid peroxidation↓, superoxide dismutase↑, glutathione peroxidase↑, catalase↑, mitochondrial lipid peroxidation and swelling↓	Guang-yin Zhou et al. & 1999 (Zhou et al., 1999)
Tanshinone I (Tan I)	Male C57BL/6 mice (18 g ± 2 g); H9c2 cells	C57BL/6 mice: DOX 5mg/kg/week *i.v.* & 4 weeks (cumulative 20 mg/kg); H9c2 cells: 1 μM DOX & 24 h	Transmission electron microscopy, H&E, Hoechst staining, DCFHDA staining, JC-1 staining, Echocardiography, DHE, western blot, immunofluorescence, MitoSOX™ Red assays, JC-1 staining assays	Myocardial structural damages↑, EF↓, FS↓, infiltration of inflammatory cells, expansion of intercellular spaces, oxidative stress↑, ROS↑, MDA↑, apoptosis↑, mitochondrial damage in mice hearts, as illustrated by mitochondrial swelling, shortening and reduction of cristae, the appearance of focal vacuoles, MMP↓	C57BL/6 mice: DOX 5mg/kg/week *i.v.* & 4 weeks + Tan I 5, 10 mg/kg/day *i.g.* & 4 weeks; H9c2 cells: 1 μM DOX & 24 h + 10 μM Tan I & 24h	p-AKT↑, Nrf2↑, HO-1↑, NQO1↑, ROS↓, myocardial structural damages↓, EF↑, FS↑, oxidative stress↓, ROS↓, MDA↓, T-SOD↑, GSH-Px↑, apoptosis↓, Bcl-2↑, Bax↓, the mitochondrial structures↑, MMP↑	Qianqian Jiang et al. & 2022 (Jiang et al., 2022b)
	Male C57BL/6 mice (18 g ± 2 g)	DOX 6 mg/kg *i.v.* & on day 6 and day 9	Echocardiography, immunofluorescence, western blot, H&E, DCFH-DA stainning	Cardiac function↓, LVEF↓, LVFS↓, LVIDs↑, CK-MB↑, LDH↑, SOD↓, GSH-Px↓, MDA↑, p-Akt↓, Nrf2↓, HO-1↓, NQO1↓, ROS↑	DOX 6 mg/kg *i.v.* & 6,9 day Tan I 10 mg/kg *i.p.* & 12 days	Cardiac function↑, LVEF↑, LVFS↑, LVIDs↓, CK-MB↓, LDH↓, SOD↑, GSH-Px↑, MDA↓, Nrf2↑, p-Akt↑, Nrf2↑, HO-1↑, NQO1↑, Akt-Nrf2 pathway↑, ROS↓	Qianqian Jiang et al. & 2022 (Jiang et al., 2022a)
Salvianolic acid A (Sal A)	H9c2 cells	DOX (0, 1, 2, 4, 8 μM) & 12 h	Cell Counting Kit-8, TUNEL staining, western blot, Luciferase Reporter Assay, Real-Time qPCR, Chromatin Immunoprecipitation Assay	Cell viability↓, apoptosis↑, caspase-3/9↑, Bcl-2↓, TUNEL-positive cells↑, NF-κB signaling↑, p-IkBa↑, p-IKKa↑, p-IKKb↑ p65/p50↑, NFKB1 mRNA and nuclear expression↑, PVT1↑	DOX 4 μM + Sal A (0, 2, 10 and 50 μM) & 12 h	Cell viability↑, caspase-3/9↓, Bcl-2↑, TUNEL-positive cells↓, NF-κB signaling↓, p-IkBa↓, p-IKKa↓, p-IKKb↓, p65/p50↓, NFKB1 mRNA and nuclear expression↓, PVT1↓	Yumeng Wu et al. & 2021 (Wu et al., 2021)
Salvianolic acid B (Sal B)	Male SD rats (200-220 g); primary adult SD rat ventricular myocytes	SD rats:DOX 3 mg/kg every two days *i.p.* & 6 days; ventricular myocytes:DOX 1 μm & 4h	H&E, TUNEL Staining, Soft Edge MyoCam system, JC-1 staining assay, Fura-2/AM staining, western blot, JC-1 staining	Cardiotoxicity↑, body and heart weights↓, LDH↑, cytoplasmic vacuolisation, myofibrillar loss, mitochondrial oedema, chromatin condensation cardiomyocyte necrosis, cardiomyocyte apoptosis↑, cardiomyocyte contractile dysfunction↑, intracellular Ca^{2+} handling derangement↑, $\Delta\Psi m$ in Adult rat ventricular myocytes↓, ERS↑, GRP78↑, CHOP↑, TRPC3↑, TRPC6↑	SD rats:Sal B (0.25, 0.5 and 1mg/kg *i.v.*) & 7 days + DOX 3 mg/kg every 2 days *i.p.* & 6 days; ventricular myocytes: Sal B 20 μg/ml & 6 h + DOX 1 μm & 4 h	TUNEL-positive cells↓, apoptotic damage↓, body and heart weights recovery, cardiomyocyte contractile dysfunction↓, intracellular Ca^{2+} handling derangement↓, $\Delta\Psi m$ in Adult rat ventricular myocytes↑, ERS↓, GRP78↑, CHOP↓, TRPC3↓,TRPC6↓	Rongchang Chen et al. & 2017 (Chen et al., 2017)
	Male BALB/c mice (6,8 weeks old)	DOX 20 mg/kg *i.p.* & single	Echocardiographic measurements, ECG, Electron microscopy, TUNEL staining, western blot	Body weight↓, heart dysfunction↑, cardiac function↓, EF↓, FS↓, LVIDd↑, LVIDs↑, LDH↑, CK↑, AST↑, heart tissue abnormities, such as cytoplasmic vacuolisation, myofibrillar loss, mitochondrial oedema, chromatin condensation	Sal B 2 mg/kg *i.v.* & 7 day followed by DOX 20 mg/kg *i.p.*	Body weight↑,heart dysfunction↓, cardiac function↑, EF↑, FS↑, LVIDs↓, LVIDs↓, LDH↓, CK↓, AST↓, heart tissue abnormities, such as cytoplasmic vacuolisation↓, myofibrillar loss↓, mitochondrial oedema↓, chromatin	Rongchang Chen et al. & 2016 (Chen et al., 2016)

(*continued on next page*)

Table 2 (*continued*)

Active component	Model	DOX dosage & protocol of usage; administration route	Detection methods & technology	Outcomes of DOX on cardiac cells/ tissue	Danshen dosage & protocol of usage; administration route	Danshen coadministration outcomes	Author & year
				and cardiomyocyte necrosis, apoptosis↑, caspase-3 and caspase-12↑, Bcl2/Bax↓, GRP78 and CHOP↑, p-IRE1↑, p-JNK↑, ATF6↑, p-PERK↑, myocardial phospho-Akt↓, phospho-GSK-3β↓		condensation↓, cardiomyocyte necrosis↓, apoptosis↓, caspase-3↓, caspase-12↓, Bcl2/Bax↑, GRP78↓, CHOP↓, p-IRE1↓, p-JNK↓, ATF6↓, p-PERK↓, myocardial phospho-Akt↑, phospho-GSK-3β↑	
Salvianolic acid C (Sal C)	H9c2 cells	DOX 0.5 μM & 48 h	CCK-8, LDH assay, microscopy, TUNEL staining, flow cytometry (Annexin V-FITC/PI), Western blotting, DCFH-DA probe, detection of MDA, SOD, GSH levels, network pharmacology, molecular docking, proteomic analysis	Myocardial viability↓, LDH↑, cell morphology damage (rounded and floated), apoptosis↑, ROS↑, MDA↑, SOD↓, GSH↓, p-PI3K↓, p-AKT↓, p-mTOR↓, p-JNK↑, Nrf2↓, HO-1↓, Bcl-2/Bax ratio↓, cleaved caspase-3↑	DOX 0.5 μM+Sal C 100 μM & 48 h	Myocardial viability↑, LDH↓, cell morphology improved, apoptosis↓, ROS↓, MDA↓, SOD↑, GSH↑, p-PI3K↑, p-AKT↑, p-mTOR↑, p-JNK↓, Nrf2↑, HO-1↑, Bcl-2/Bax ratio↑, cleaved caspase-3↓	Siqi Chen, Chenchen Jiang, et al. & 2025(Chen et al., 2025)
Cryptotanshinone (CPT)	H9c2 cells	DOX 1 μM & 24h	Immunoprecipitation assay, CCK-8, Hoechst 33342 staining, western blot, Calcein-AM staining, JC-1 Assay	Cell viability↓, ROS↑, apoptosis↑, mitochondrial membrane integrity↓, phosphorylated levels of Akt↓, GSK-3↓, GSK-3β-ANT interaction↓, ANT-CypD complex↑	DOX 1 μM & 24 h + CPT (5, 10 and 25 μM) co-treat & 24h	Cell viability↑, ROS↓, apoptosis↓, mitochondrial membrane integrity↑, phosphorylated levels of Akt and GSK-3β↑, GSK-3β-ANT interaction↑, ANT-CypD complex↓	Xiaoping Wang et al. & 2021 (Wang et al., 2021a)
	Male Wistar rats (220-260 g); H9c2 cells	Wistar rats: DOX 2mg/kg *i.p.* & every other day & 2 weeks; H9c2 cells: DOX 2 μM & (3,6 and 12 h)	CCK-8, F-actin staining, flow cytometry, echocardiography, hemodynamic evaluation, transcriptomic profiling, bioinformatics analysis, TUNEL, western blot	Apoptosis↑, cardiac function↓, collagen↑, ROS↑, MDA↑, EF↓, FS↓, left shift of the pressure-volume (PV) loop, cavities were found in the nucleus, the cardiomyoblast were loosely aligned, the surface areas of the cardiomyoblast↓, collagen deposition in the hearts of rats, cardiac collagen↑, JNK↑, PI3 kinase↓, p85↓, p-AKT↓, cytoplasmic p53 and Foxo1 were significantly translocated to the nucleus in the cardiomyocytes,Bcl-2↓, Bcl-xl↓, Bak↑, Bim↑, PUMA↑, 14-3-3σ↑	Wistar rats: DOX 2mg/kg *i.p.* every other day & 2 weeks + CPT 50 mg/kg *p.o.* & once every 2 days & 6 weeks; H9c2 cells: DOX 2 μM + CPT (2, 5 and 10 μM) & 3,6,12 h	Apoptosis↓, cardiac function↑collagen ↓, ROS↓, p53 signaling pathway↓, right shift of the PV loop along the horizontal axis, the number of hollow nuclei↓, the cardiomyoblast were more tightly aligned, the surface areas of the cardiomyoblast significantly increased↑, SOD↑, CAT↑, MDA↓, GSH-Px↑, JNK↓, PI3 kinase↑, p85↑, p-AKT↑, Bcl-2↑, Bcl-xl↑, Bak↓, Bim↓, PUMA↓, caspase-9↓, caspase-3↓, suppressed p53 nuclear translocation and enhanced Foxo1 nuclear retention,14-3-3σ↓	Le Li et al. & 2020 (Li et al., 2020)
	Adult male Wistar rats (300 ± 50 g)	DOX 1.25 mg/kg *i.p.* every other day (begin day 9)& 12 days	ELISA, (JC-1) staining, Real-time qPCR, reverse-phase HPLC, Chemical colorimetry, reverse-phase highpressure liquid chromatography	ATP generation↓, The activity of complexes I, III and IV↓, MMP↓, superoxide↑, PGC-1a↓, NRF-1↓, TFAM↓, Mitochondria damage↑, Oxidative stress↑, Mitochondrial biogenesis↓, NO↑, iNOS↓, GSH-PX↓, superoxide anion free radicals↑,	DOX 1.25 mg/kg *i.p.* every other day & 12 days (begin day 9) + CPT 50 mg/kg *p.o.* & 20 days	ATP generation↑, The activity of complexes I, III and IV↑, Mitochondria damage↓, Oxidative stress↓, Mitochondrial biogenesis↑, NO↓, iNOS↑, GSH-PX↑, PGC-1a↑, NRF-1↑, TFAM↑, superoxide anion free radicals↓, expressions of mitochondrial biogenesis-related genes↑	Yanshan Zhang et al. & 2016 (Zhang et al., 2016b)
Ferulic acid (FA)	Adult male Wistar rats (250–300 g)	DOX 20 mg/kg *i.p.* & on day 5	Automated biochemistry analyzer, ECG, Atomic absorption spectroscopy, colorimetry, RT-PCR, western blot, Masson's trichrome staining	RR↑, QTc interval↑, QRS complex↑,CK-MB↑, LDH↑, IL-1β↑, IL-6↑,Ca^{2+}↑, Mg^{2+}↑, ATPase↑, Ca^{2+} ATPase↑, ANP↑ and BNP↑	DOX 20 mg/kg *i.p.*+ FA (20 mg/kg and 40 mg/kg, *p.o.*) & 7 days	ECG was normal, CK-MB, LDH, IL-1β and IL-6 were not elevated, ANP and BNP↓, myocardial GSH and Na^{+}/K^{+} ATPase↑	Urmila Aswar et al. & 2019 (Aswar et al., 2019)
	H9c2 cells	DOX 1 μmol/L & 24h	CCK-8, phase contrast microscope, DCF-DA staining with flow cytometry, AO-EB staining, DNA agarose gel electrophoresis, Western blot	Cell viability↓, apoptosis↑, ROS↑, LDH↑, CK↑, MDA↑, SOD↓, caspase-3↑, Bax↑, Bcl-2↓	FA (10, 20 and 40) μmol/L & 2 h + DOX 1 μmol/L & co-treated 24h	Cell viability↑, LDH↓, CK↓, reversed morphological changes, ROS↓, MDA↓, SOD↑, caspase-3↓, Bax↓, Bcl-2↑	Zhijuan. Wu et al. & 2014 (Wu et al., 2014)

(*continued on next page*)

Table 2 (*continued*)

Active component	Model	DOX dosage & protocol of usage; administration route	Detection methods & technology	Outcomes of DOX on cardiac cells/ tissue	Danshen dosage & protocol of usage; administration route	Danshen coadministration outcomes	Author & year
Danshensu (DSS)	Adult male KM mice (18–21 g)	DOX 15 mg/kg *i.p.* injected 6 h after normal saline injection in days 4–7	ECG, H&E, Serum Biochemical Analysis, ELISA, Western Blotting	CK↑, LDH↑, Bcl-2↓, caspase-3↑, ROS↑, Keap↑, IL-6↑, TNF-α↑, MDA↑, CAT↓, GPX↓, SOD↓, BAX↑, HO-1↓, NQO1↓, Nrf2 ↓	DOX 15mg/kg & 6 h after protective drug injection in days 4–7 + DSS 50 and 100 mg/kg *i.p.* & 7 days; CAP: DOX 15mg/kg & 6 h after protective drug injection in days 4–7 + CAP 45 mg/kg *i.p.* & 7 days	CK↓, LDH↓, Bcl-2↑, caspase-3↓, ROS↓, Keap↓, IL-6↓, TNF-α↓, MDA↓, CAT↑, GPX↑, SOD↑, Bax↓, HO-1↑, NQO1↑, Nrf2 ↑	Jiaying Qi et al. & 2022 (Qi et al., 2022)
Dihydrotanshinone I (DHT)	Zebrafish (1–3 dpf); Male C57BL/6 mice (18 g ± 2 g); H9c2 cells	Zebrafish: DOX 100 μM & 3 dpf; C57BL/6 mice: DOX *i.v.* 5 mg/kg once a week & 4 weeks; H9C2 cells:DOX 1 μM & 24h	Echocardiography, histological examination, H&E, flow cytometry, immunochemistry, western blot, immunofluorescence	Pericardial edema↑, tail blood accumulation↑, heart structure damage, blood flow↓, heart rate↓, survival rate↓.EF↓, FS↓, LVEDD↑, LVESD↑, M1 macrophages↑, pro-inflammatory↑, NF-κB↑, nuclear expression of TFEB↓, p-IKKα/β↑, COX2↑, TNF-α↑, p-NF-κB↑	Zebrafish: DOX 100 μM + 10 nM DHT & 3 dpf; C57BL/6 mice: DOX 5 mg/kg *i.v.* once a week & 4 weeks + DHT 20 mg/kg *i.p.* & 4 weeks (1 week post-last DOX); H9c2 cells: DOX 1 μM + DHT 10 nM & 24h	Pericardial edema↓, tail blood accumulation↓, heart structure damage↓, blood flow↑, heart rate↑, survival rate↓.EF↓, FS↓, LVEDD↓, LVESD↓, M1 macrophages↓, pro-inflammatory↓, activation and nuclear localization of NF-κB↓, nuclear expression of TFEB↑, p-IKKα/β↓, COX2↓, TNF-α↓, p-NF-κB↓	Xiaoping Wang et al. & 2020 (Wang et al., 2020a)
Diethyl blechnic (DB)	Primary cultured neonatal SD rat cardiomyocytes; H9c2 cells	DOX 1 μM & 24h	MTT, JC-1 staining, Hoechst 33342 staining, TUNEL, western blot	Cell death↑, apoptosis↑, Bcl-2↓, Bcl-xl↓, caspase-3/7/8/9↑, ROS↑, MAPKs signaling↑, p-JNK1/2↑, p-ERK1/2↑, p-p38↑.	DOX 1 μM & 24h+DB (0, 5, 10, 20 and 40 μM) & 24 h; DB 20 μM pre-treated 2 h + DOX co-treated 1 μM & 24 h; DB (0,5,10 and 20 μM) + DOX 1 μM & 24 h	Cell Death↓, apoptosis↓, Bcl-2↑, Bax↓, p-p53↓, cyt c↓, caspase-3/7/8/9↓, oxidative Stress↓, p-JNK1/2↑	Jie Yu et al. & 2018 (Yu et al., 2018a)
Compound DanShen Dripping Pill (CDDP)	Male C57BL/6 mice (~8-week-old); H9c2 cells	C57BL/6 mice: DOX 5 mg/kg *i.p.* once weekly & 4 weeks; H9c2 cells: DOX 1 μM & 24h	ECG, Echocardiography, Serum Biochemical Assay, H&E, TUNEL, RNAseq, qRT-PCR, Western blot, CCK-8, OGD	Cardiac atrophy and heart dysfunction↑, cardiac fibrosis and inflammation↑, oxidative stress↑, apoptosis↑, metabolic disorders↑	C57BL/6 mice: DOX 5mg/kg *i.p.* weekly + 660 mpk CDDP (L) *p.o.* (3 days prior & ongoing) & 4 weeks; DOX 5mg/kg *i.p.* weekly + 2640 mpk CDDP(H) *p.o.* (3 days prior & ongoing) & 4 weeks; H9c2 cells: DOX 1 μM & 24 h + CDDP(200 and 500 μg/mL) & 24 and 48 h	Cardiac atrophy and heart dysfunction↓, cardiac fibrosis and inflammation↓,oxidative, stress↓, apoptosis↓, metabolic disorders↓	Ke Feng et al. & 2021 (Feng et al., 2021)
Danhong injection (DHI)	Male SD rats (200 ± 20 g); Primary cultured neonatal SD rat cardiomyocytes	SD rats: DOX 2.5 mg/kg *i.p.* every other day & 6 days; cardiomyocytes: DOX 0.9 μM & 48h	HPLC−ESI-Q-TOF-MS/MS, histopathological examination, oxidative stress markers assay, Network pharmacology analysis, Molecular docking verification AutoDockTools, western blot, ECG, automatic biochemical blood analyzer	BW↓, HW↓, ECG↓, serum biochemical indicators levels↑, cardiac oxidative enzymes↓	SD rats:DOX 2.5 mg/kg *i.p.* (4, 6, 8, 10, 12 and 14 days) + DHI 4.16 ml/kg *i.v.* & 14 days; cardiomyocytes: DOX 0.9 μM + DHI 10μL/mL & 48h	BW↑, HW↑, ECG↑, serum biochemical indicators levels↓, cardiac oxidative enzymes↑	Xiaojiao Yi et al. & 2022 (Yi et al., 2022)
Salvianolic acids (SA)	Zebrafish Tg (myl7: mRFP-EGFP-LC3)	DOX 25 mg/L (28 hpf to 72 hpf)	RNA-seq, TUNEL assay, EGFP/mRFP-LC3 imaging (autophagic flux), qRT-PCR, Western blot, luciferase assay	Pericardial edema↑, heart rate↓, apoptosis↑, autophagosomes↓, autolysosomes↓, miR-30a↑, becn1 mRNA/protein↓	DOX 25 mg/L (28 hpf to 72 hpf); +SA 0.4 g/L & (28 hpf to 72 hpf)	Pericardial edema↓, heart rate↑, apoptosis↓, miR-30a↓, beclin1 mRNA/protein↑	Jianxuan Li et al. & 2024 (Li et al., 2024a)
	Adult male KM mice (20–25 g)	DOX 5mg/kg *i.p.* & 3 days	ORAC, Lowry method CK MDA, H&E, ECG	MDA↑, serum CK↑, HW/TL↓, creatine kinase↑, electrocardiography↓, heart vacuolation↓, oxidative stress↑	DOX 15 mg/kg *i.p.* on day 1+ SA 40 mg/kg *i.p.* & 3 days	MDA↓, serum CK↓, HW/TL↑, creatine kinase↓, electrocardiography↑, heart vacuolation↑, oxidative stress↓	Baohong Jiang et al. & 2008 (Jiang et al., 2008)

(*continued on next page*)

Table 2 (*continued*)

Active component	Model	DOX dosage & protocol of usage; administration route	Detection methods & technology	Outcomes of DOX on cardiac cells/ tissue	Danshen dosage & protocol of usage; administration route	Danshen coadministration outcomes	Author & year
Salvia miltiorrhiza aqueous extract (SMAE)	Male Wistar rats (250–300 g); H9c2 cells	Wistar rats:DOX 3 mg/kg *i.p.* & 6 doses/ 2 weeks; H9c2 cells: DOX 1 μM & 24 h	IHC, TUNEL, 2-D PAGE, Derivatization of Protein Carbonyls and DNP Immunostaining,In-Gel Enzymatic Digestion and Mass Spectrometry, Biological Network Analysis Using MetaCore™, MTT, Western Blot	Cell death↑, apoptosis↑, Bcl-2↓, Bcl-xl↓, caspase-3↑, ROS↑, Nrf-2↓, Catalase SOD↓, ERK/p53/Bcl-xL/ caspase-3 signaling pathways and the mitochondrial dysfunction	Wistar rats:DOX 3 mg/kg & 6 doses/2 weeks + 100 mg/ kg/day of SMAE *p.o.* & (during and 5 weeks post-DOX); H9c2 cells: DOX 1 μM + SMAE (0, 1.25 and 2.5) mg/kg & 24 h	Detoxifying enzyme systems↑, ROS↓, Nrf2↑, HO-1 ↑, Catalase SOD↑, amended the ERK/p53/Bcl-xL/ caspase-3 signaling pathways and the mitochondrial dysfunction	YuChiang Hung et al. & 2020 (Hung et al., 2020)
	Male Wistar rats (250–300 g)	DOX 3 mg/kg *i.p.* three times per week & 2 weeks	Hemodynamic measurements, biochemical analyses of serum, synthesis rates of DNA, RNA and protein, myocardial antioxidants, lipid peroxidation, histopathological procedure	Liver function↓, Nucleic acid↓, protein synthesis↓, lipid peroxidation↑, GSHPx activity↓, SOD↓, myocardial lesions↓, cardiac and hepatic toxicity↑	DOX 3 mg/kg *i.p.*+ SMAE 20 and 100 mg/kg *p.o.* & 30 days	Liver function↑, Nucleic acid↑, protein synthesis↑, lipid peroxidation↓, GSHPx activity↑, SOD↑, myocardial lesions↑, cardiac and hepatic toxicity↓	JyhSheng You et al. & 2007 (You et al., 2007)
Qiliqiangxin (QL)	Male Wistar rats (180–200 g)	DOX 2.5 mg/kg/ week *i.p.* & 6 weeks.	H&E, IHC, ELISA, qRT-PCR, Western blot, miRNA-seq and bioinformatics, miRNA target luciferase reporter assay, HEK 293 cell culture and transfection	Apoptosis↑, inflammation↑, fibrosis↑, TGF-b1/Smad3 signalling pathway↑, TGF-b3/ Smad7 signalling pathway↓	DOX 2.5 mg/kg/week & 6 weeks *i.p.* + QL (1.0 g/kg/d) *p.o.* & 4 weeks	Apoptosis↓, inflammation↓, fibrosis↓, promoted neovascularization, TGF-b1/ Smad3 signalling pathway↓, TGF-b3/Smad7 signalling pathway↑	Xutao Sun et al. & 2020 (Sun et al., 2020)
Herbal formula B307 (B307)	Male ICR mice (20 weeks)	DOX 10 mg/kg *i.p.* 2 injections separated & 3 days	Echocardiography, immunohistochemistry, western blot, H&E	Mortality rate↑, body weight↓, cardiac function↓, endothelial nitric oxide synthase↓, superoxide dismutase 2↓, B-cell lymphoma 2↓, ROS↑, NFKB1 (p50 and its precursor, p105)↑, neurotrophin-3↑, Bcl-2-associated X protein↑, calpain↑, caspase-12↑, caspase-9↑, caspase-3↑,	B307 (50 mg/kg *p.o.*) & 14 days + DOX (10 mg/kg; *i.p.*) & 2 times separated by 3 days	Mortality rate↓, body weight↑, cardiac function↑, endothelial nitric oxide synthase↑, superoxide dismutase 2↑, B-cell lymphoma 2↑, NFKB1 (p50 and its precursor, p105)↓, neurotrophin-3↓, Bcl-2-associated X protein↓, calpain↓, caspase-12↓, caspase-9↓, caspase-3↓, ROS↓	Chiaying Lien et al. & 2015 (Lien et al., 2015)
Qishen granule (QSG)	Male C57BL/6 mice (20±2 g); H9c2 cells	C57BL/6 mice: DOX6 mg/kg *i.v.* on day 6 and 9; H9c2 cells: DOX (0.1-2 μmol/L) & 24 h	Echocardiography,CK-MB, LDH, SOD, MDA, Histopathologic assay, TUNEL staining,DCFH-DA staining and MitoSOX red reagents, JC-1, ATP, Western blot	Cardiac function↓, EF↓, FS↓, MDA↑, SOD↓, protein acetylation↑, SIRT3↓, Ac-SOD↑, mitochondrial membrane potential↓, ATP↓, ROS↑	C57BL/6 mice: QSG (2.5 g/ kg and 5 g/kg) *i.g.* and pravastatin (40 mg/kg) & 14 days+DOX 6 mg/kg *i.v.* on day 6 and 9; H9c2 cells: pre-treated with QSG 25-1200 μg/ml & 24 h+ co-exposure with 1 μM DOX & 24 h	Cardiac function↑, EF↑, FS↑, MDA↓, SOD↑, protein acetylation↓, SIRT3↑, Ac-SOD↓, mitochondrial membrane potential↑, ATP↑, ROS↓	Jingmei Zhang et al. & 2024 (Zhang et al., 2024)
	Male C57BL/6 mice (20 g ± 2 g); H9c2 cells	C57BL/6 mice 6 mg/ kg (on day 6 and 9) *i.v.*; H9c2 cells:1 μM DOX & 24 h	Echocardiography, TEM, DHE staining, GSH/MDA assays, immunofluorescence, Western blot, siRNA transfection, MitoSOX/ FerroOrange staining	EF↓, FS↓, iron↑, MDA↑, GSH↓, mitochondrial vacuolation/ membrane rupture↓, ROS↑, cell death↑, TUNEL-positive cells↑	C57BL/6 mice:6 mg/kg DOX (on day 6 and 9) *i.v.*+ QSG (2.5 g/kg or 5 g/kg *i.g.* & 12 days); H9c2 cells: 1 μM DOX + 800 μg/ml QSG & 24 h	EF↑, FS↑, iron↓, MDA↓, GSH↑, ROS↓, mitochondrial integrity↑, Nrf2↑, GPX4↑, FTH1↑, cell death↓, TUNEL-positive cells↓	SimingXue et al. & 2024 (Xue et al., 2024)
Ershen Zhenwu Decoction (ESZWD)	Male SD rats (200-220 g), Primary cultured neonatal SD rat cardiomyocytes	SD rats:0.02% DOX 1 mL/100 g body weight twice weekly *i.p.*& 3 weeks	Echocardiograph, H&E/Masson/ Sirius red staining, ELISA, Western blot, qRT-PCR, UHPLC-Q-TOF-MS	LVEF↓, LVIDs↑, collagen I A1↑, α-SMA↑, mitochondrial damage↑, TNF-α↑, IL-11↑, IL-17A↑, RhoA/ ROCKs pathway↑	SD rats: 0.02% DOX (1 mL/ 100 g bodyweight twice weekly for 3 weeks *i.p.*) +ESZWD dosage: 3.96 g/kg (low), 7.92 g/kg (medium), 15.84 g/kg (high), oral gavage for 4 weeks (rats); Danshen content: 30 g in ESZWD formula (total 81.9 g)	LVEF↑, LVIDs↓,collagen I A1↓, α-SMA↓, TNF-α↓, IL-11↓, IL-17A↓, RhoA/ROCKs pathway↓	Dan Cheng et al. & 2025 (Cheng et al., 2025)

intragastric administration (i.g.), intraperitoneal injection (i.p.), intravenous injection (i.v.), per os (p.o.).

accompanied with elongated heart atria, collapsed ventricles, decreased fractional shortening (FS), reduced erythrocyte circulation in tail vessels, and declined heart rate and survival rate. DHT treatment significantly improved these parameters by increasing FS, enhancing blood flow and improving survival rates (Wang et al., 2020a). In C57BL/6 mice, after weekly DOX tail vein injections for four weeks, the left ventricular end-diastolic (LVEDD) and end-systolic diameters (LVESD) increased and FS reduced, indicating DOX decreased cardiac contractility. DHT treatment improved left ventricular function by decreasing LVEDD and LVESD and significantly increasing FS and ejection fraction (EF) (Wang et al., 2020a).

Salvianolic acids

Salvianolic acid A. Salvianolic acid A (Sal A, $C_{26}H_{22}O_{10}$) is a water-soluble phenolic acid compound extracted from *S. miltiorrhiza* (Li et al., 2018b), and has been extensively documented for its anti-apoptotic properties and cardioprotective effects. Sal A dose-dependently protected against DOX-induced inflammation, cell viability decrease and apoptosis in H9c2 cells (Wu et al., 2021).

Salvianolic acid B. Salvianolic acid B (Sal B, $C_{36}H_{30}O_{16}$), which is an abundant phenolic acid compound extracted from *S. miltiorrhiza* (Su et al., 2015), exhibits cardiovascular protective effects by promoting cardiomyocyte survival, inhibiting apoptosis and preserving normal cellular functions (Wang et al., 2011; Xu et al., 2011). DOX impaired heart contractile function, disrupted intracellular Ca^{2+} homeostasis, decreased mitochondrial membrane potential, increased endoplasmic reticulum stress (ERS), and elevated apoptosis in the cardiomyocytes of both SD rats and BALB/c mice (Sishi et al., 2013). Chen et al. also found that Sal B protected against DIC and ERS in SD rats and BALB/c mice (Chen et al., 2016). Sal B pretreatment mitigated DOX-induced reduction of body weight and heart weight, and ameliorated cardiomyocyte damage and apoptosis (Chen et al., 2017; Chen et al., 2016).

Salvianolic acid C. Salvianolic acid C (Sal C, $C_{26}H_{20}O_{10}$), a water-soluble polyphenolic compound derived from *S. miltiorrhiza* (Su et al., 2015), demonstrates significant cardioprotective effects against DIC in rat cardiomyoblast H9c2 (Chen et al., 2025). Sal C treatment dose-dependently preserved cellular viability and attenuated morphological damage in DOX-exposed cardiomyoblasts, ultimately reducing characteristic cardiotoxicity features including cell rounding and detachment. Furthermore, Sal C suppressed DOX-induced apoptosis in H9c2 cells and mitigated oxidative injury, as evidenced by reduced ROS accumulation and lipid peroxidation. Sal C also counteracted DOX-driven depletion of endogenous antioxidants SOD and glutathione (GSH) in H9c2 cells. These findings collectively indicate that Sal C protects cardiomyoblasts from DIC through inhibition of apoptosis and oxidative stress.

Others

Danshensu. Danshensu (DSS, $C_9H_{10}O_5$) is a water-soluble constituent extracted from *S. miltiorrhiza,* and it is structurally composed of catechol and lactic acid (Zhang et al., 2019). Jia-Ying Qi et al. found that DSS dose-dependently protected against DIC in KM mice along with preventing body weight loss, mortality, QTc interval prolongation, and cardiomyocyte necrosis (Qi et al., 2022). In the hearts of KM mice, DSS decreased oxidative stress markers ROS and MDA, while increasing antioxidant enzymes SOD, CAT and GPX. Additionally, DSS reduced inflammatory markers TNF-α and IL-6, and apoptotic markers Bax/Bcl-2 ratio and caspase-3. Additionally, the release of CK and LDH, which are specific markers for cardiac injury (Alam et al., 2018; Cove-Smith et al., 2014), dramatically increased in the DOX treatment group, but decreased in the DSS pretreated group. These findings indicate that DSS protects against myocardial cardiac dysfunction and structural injury in DIC models, which suggests its potential as a cardioprotective agent in chemotherapy-induced cardiac damage.

Ferulic acid. Ferulic acid (FA, $C_{10}H_{10}O_4$), which is a water-soluble ingredient isolated from *S. miltiorrhiza*, presented cardioprotective effects against DIC (Zhong et al., 2009). In the Wistar rat model, FA ameliorated DOX-induced electrocardiographic abnormalities, for example, prolonged ECG intervals (RR, QTc and QRS intervals). FA treatment obviously attenuated DOX-induced cardiac dysfunction which was evidenced by the reduction in blood pressure and normalization of heart rate. FA administration markedly decreased the serum levels of cardiac injury markers (CK-MB and LDH) and downregulated the expression of pro-inflammatory cytokines (IL-1β and IL-6) in the Wistar rat model (Aswar et al., 2019). Moreover, FA reduced collagen deposition and fibrosis associated with DOX-induced interstitial cardiac fibrosis. FA increased the activity of antioxidant factor GSH and Na^+/K^+ ATPase activities (Chen et al., 2010; Kania et al., 2009). FA partially reversed the DOX-induced cell viability reduction, morphological change and LDH and CK release in rat cardiomyoblast H9c2 (Aswar et al., 2019; Wu et al., 2014). Furthermore, FA inhibited DOX-induced ROS and MDA production, while enhancing SOD activity. FA reduced the expression of apoptotic markers, caspase-3 and Bax, and up-regulated anti-apoptotic marker Bcl-2 (Aswar et al., 2019; Wu et al., 2014). These findings suggest that FA might serve as a promising cardioprotective agent for the prevention of DIC.

Tanshinone IIA sodium sulfonate. Sodium tanshinone IIA sulfonate (STS, $C_{19}H_{17}NaO_6S$), a water-soluble derivative of tanshinone IIA, protected against DIC in multiple mouse models (BALB c, KM and SD) and cardiomyocytes (Ji et al., 2000). STS prevented DOX-induced cellular damage through suppression of lipid peroxidation and enhancement of antioxidant enzyme activities (SOD, glutathione peroxidase, catalase) in H9c2 cells. STS inhibited DOX-induced mitochondrial lipid peroxidation and swelling and scavenged DOX semiquinone free radical in a dose-dependent manner (Jiang et al., 2009; Zhou et al., 2002; Zhou et al., 1999). Furthermore, STS improved cardiac parameters, including ECG intervals, myocardial tissue morphology and tensile strength, and reduced cardiac fibrosis (Jiang et al., 2009; Zhou et al., 2002). Thus, STS offers comprehensive protection against DOX-induced cardiac damage by combining direct radical scavenging with activation of cellular antioxidant pathways, thereby preserving mitochondrial and cardiomyocyte structural and functional integrity.

Diethyl Blechnic. Diethyl Blechnic (DB, $C_{22}H_{22}O_8$), which is a novel compound isolated from the *S. miltiorrhiza* (Gao et al., 2016). DB significantly enhanced cell viability and prevented DOX-induced death in both H9c2 cells and primary cultured cardiomyocytes in a concentration-dependent manner (Yu et al., 2018a). DB protected cardiac cells by preserving mitochondrial membrane potential and preventing DOX-induced morphological changes that associated with apoptosis (Childs et al., 2002; Yu et al., 2018a).

The extracts of Danshen prevent doxorubicin-induced cardiotoxicity

S. miltiorrhiza aqueous extract. S. miltiorrhiza aqueous extract (SMAE), which is a water-soluble preparation extracted from *S. miltiorrhiza*, demonstrated significant cardioprotective effects against DIC (Li et al., 2018b; Ren et al., 2019). Histopathological analysis showed that SMAE co-treatment significantly alleviated DOX-induced cardiac damage, preventing collagen accumulation and maintaining normal heart tissue morphology (You et al., 2007). SMAE exhibited potent antioxidant effects in cardiomyoblast H9c2. Pre-treatment with SMAE significantly enhanced cell viability and maintained mitochondrial membrane potential in DOX-treated cells. SMAE restored antioxidant enzyme

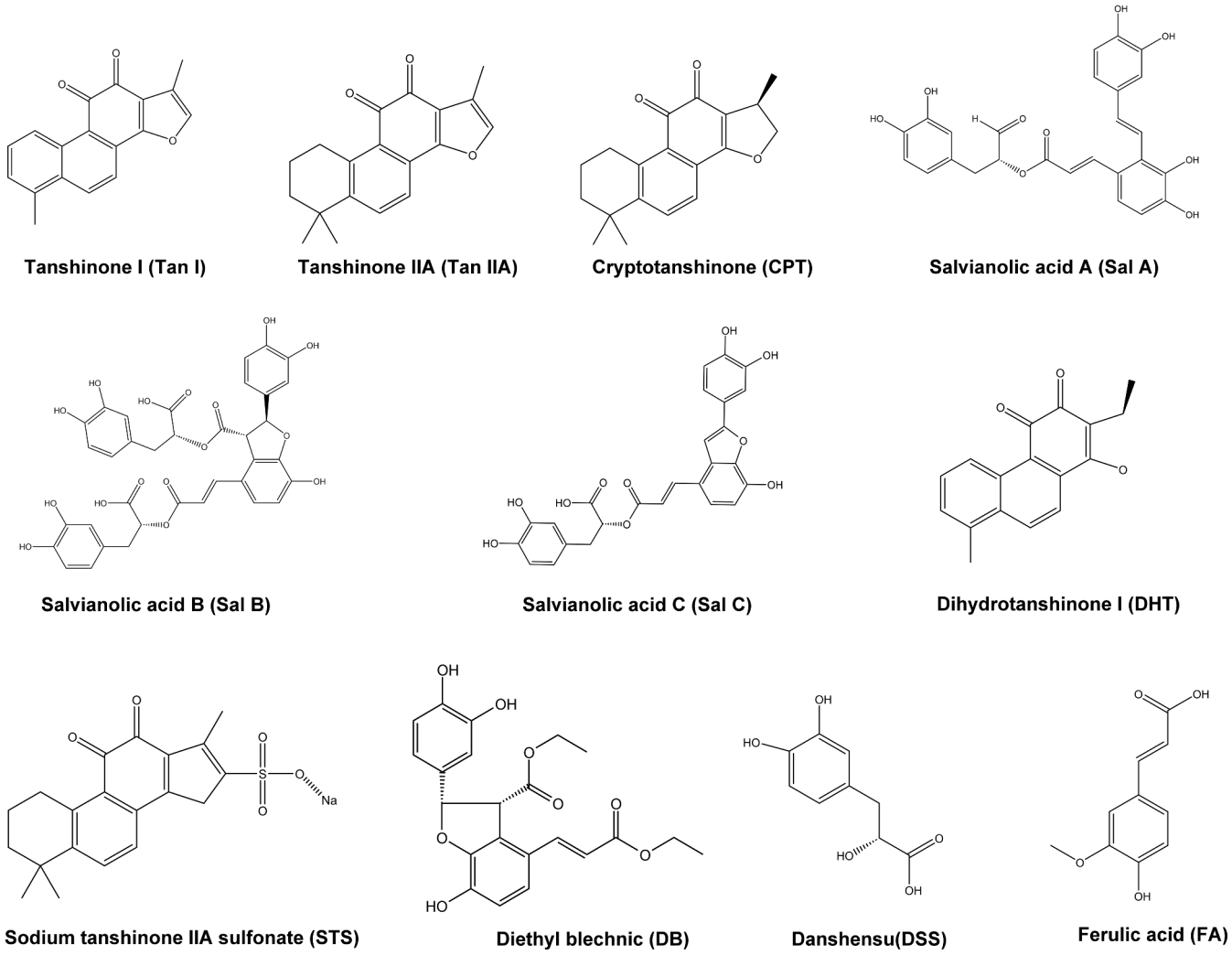

Fig. 2. The chemical structures of compounds and their derivatives which are isolated from *S. miltiorrhiza* with protective activity against DIC.

activities (SOD, GSHPx and catalase) and reduced lipid peroxidation in DOX-treated H9c2 cells (Hung et al., 2020). Flow cytometry analysis with DCF fluorescence revealed that pre-treatment with SMAE markedly reduced DOX-induced intracellular ROS generation while preserving mitochondrial function (Songbo et al., 2019; Stěrba et al., 2013). DOX exposure induced oxidative modification of specific mitochondrial proteins that are involved in critical metabolic processes (Lennicke et al., 2016). According to the results from proteomic analysis, proteins in the TCA cycle, glyoxylate and dicarboxylate metabolism were largely impaired due to ROS-mediated carbonylation and subsequent mitochondrial dysfunction (Sun et al., 2015; Wenningmann et al., 2019). These results indicate that SMAE treatment effectively reduced the carbonylation of these key metabolic proteins, thereby preserving mitochondrial function and cellular energy metabolism in DIC.

Salvianolic acids. Salvianolic acids (SA) is extracted and purified from *S. miltiorrhiza* using methanol extraction (Ma et al., 2019). The oxygen radicals absorbance capacities (ORAC) assay revealed that SA exhibited potent free radical scavenging activity in a dose-dependent manner. In cardiomyoblast H9c2 and primary cultured cardiomyocytes, SA treatment effectively attenuated DOX-induced oxidative stress (Jiang et al., 2008). SA co-treatment significantly improved DOX-induced cardiac dysfunction, which was reflected by increased heart weight/tibia length ratio and reduced serum creatine kinase levels in KM mice (Jiang et al., 2008). Electrocardiographic analysis showed that SA treatment effectively prevented DOX-induced ST interval prolongation. Histopathological examination revealed that SA substantially alleviated DOX-induced cardiac structural damage and reduced myocardial vacuolation. Furthermore, SA enhanced antioxidant capacity and attenuated lipid peroxidation in cardiac tissues, suggesting that these protective effects are mediated by modulation of oxidative stress. In zebrafish, SA decreased the DOX-caused mortality rate, reduced DOX-induced pericardial edema by over 50% and restored the heart rate to almost normal levels, which might be related to the enhancement of autophagic flux with increased formation of autolysosomes and reduced accumulation of damaged intracellular components (Li et al., 2024a).

Danshen-contained formulas ameliorate doxorubicin-induced cardiotoxicity

Compound Danshen dripping pill. The Compound Danshen Dripping Pill (CDDP, Dantonic®, T89, Fufang Danshen Diwan in Chinese) is a commercially available traditional Chinese medicine preparation, which is also known as Chinese patent medicine (CPM), which combines traditional medicine and modern medical technologies (Zhou et al., 2016). CDDP contains three medicinal herbs: *S. Miltiorrhizae,* notoginseng and borneol (Guo et al., 2016). CDDP ameliorated DOX-induced pathological changes of heart weight, left ventricular EF/FS, fibrogenesis and HF indices in C57BL/6 mice (Feng et al., 2021). CDDP significantly enhanced cell viability and mitigated DOX-induced death in both rat cardiomyoblast H9c2 and NovoCellTM-Cardiomyocytes in a

concentration-dependent manner. CDDP also ameliorated DOX-induced cardiomyocyte apoptosis and reduced the release of cardiac injury markers, including CK, LDH, BNP and NT-proBNP (Guo et al., 2016). Thus, we could conclude that CDDP potentially protects against DIC through multiple pathways.

Danhong injection. The Danhong injection (DHI) is also a CPM, which consists of *S. miltiorrhiza* and *Carthamus tinctorius,* and used to treat cardiovascular diseases in China (Feng et al., 2019; Wang et al., 2021b). Xiaojiao et al. found that DHI alleviated reductions of body weight, heart weight and cardiac function, attenuated the DOX-induced the elevation of serum heart injury markers (CK-MB and LDH) and improved the heart pathological changes in DOX-treated SD rats (Yi et al., 2022). In H9c2 cells, DHI significantly downregulated the protein expression of pro-apoptotic proteins Bax and caspase-3 and upregulated the anti-apoptotic protein Bcl-2. DHI also inhibits the mitochondria-mediated apoptotic pathway, which is typically activated by DOX-induced oxidative stress (Yi et al., 2022). DHI attenuated oxidative injury by reversing DOX-induced elevation of MDA and reduction of antioxidant enzymes SOD and GSH-Px in rat hearts (Yi et al., 2022). DHI may also restore DOX-triggered mitochondrial ROS production and redox balance by acting on predicted targets like SOD1 and NOS3 (Feng et al., 2019; Yi et al., 2022).

Qiliqiangxin capsule. The Qiliqiangxin (QL) capsule contains a combination of ingredients including Ginseng (*Panax ginseng* Radix), Huangqi (*Astragalus membranaceus* Bge) and Danshen (*S. miltiorrhiza*) that exist cardiovascular protection and antioxidant activities (Tang and Huang, 2013; Zou et al., 2012). DOX caused cardiac dysfunction, remodeling, inflammation, apoptosis and fibrosis in Wistar rats while QL markedly enhanced cardiac performance by increasing EF, FS, LVSP, +dp/dtmax and -dp/dtmax and decreasing LVIDd, LVIDs and LVEDP compared to the DOX-treated group (Sun et al., 2020). These results support that QL might be an effective treatment for DIC.

Herbal formula B307. The herbal formula B307, which contains ingredients like Ginseng (*Panax ginseng Radix*) and Danshen (*S. miltiorrhiza*) etc., demonstrates significant cardioprotective effects against DIC (Lien et al., 2015). B307 improved the survival rate, body weight, cardiac function and microcirculation in Institute of Cancer Research (ICR) mice compared to DOX-treated group. B307 suppressed oxidative stress, inflammation and apoptosis in the heart tissue of DOX-treated ICR mice by increasing antioxidant enzymes, reducing inflammatory cytokines and inhibiting apoptotic signaling (Lien et al., 2015).

Qishen granules. The CPM Qishen Granules (QSG) was derived from the classic formula 'Zhen-Wu-Tang', which has been extensively used in the treatment of myocardial infarction in Chinese medicine (Li et al., 2016a). QSG consists of six traditional Chinese herb medicines, including *Astragalus membranaceus* var. *mongholicus* (Bunge) P.K.Hsiao (Fabaceae), *S. miltiorrhiza* Bunge (Lamiaceae), *Lonicera japonica* Thunb. (Caprifoliaceae), *Aconitum carmichaelii* Debeaux (Ranunculaceae), *Scrophularia ningpoensis* Hemsl. (Scrophulariaceae) and *Glycyrrhiza uralensis* Fisch. (Fabaceae). QSG treatment improved cardiac function by increasing EF and FS, while reduced serum cardiac damage markers CK-MB and LDH in DOX-treated C57BL/6 mice. QSG also prevented heart tissue structure impairment, decreased oxidative stress and reduced cardiomyocyte apoptosis (Zhang et al., 2024). QSG reduced myocardial structural damage by diminishing inflammatory infiltration and preserving cardiomyocyte morphology. QSG protected against DOX-induced mitochondrial damage by reducing vacuolation and cristae disruption. Complementary *in vitro* experiments showed that QSG improved cell viability, reduced ROS levels and protected mitochondrial function by increasing membrane potential and ATP production in cardiomyoblast H9c2. Both *in vivo* and *in vitro* studies consistently demonstrated that QSG's cardioprotective effects, which provide an experimental basis for QSG's potential as a treatment for DIC.

Ershen zhenwu decoction. The CPM Ershen Zhenwu Decoction (ESZWD) is formulated based on the classic Chinese medicinal formula known as Zhenwu Decoction, which originates from the 'Treatise on Typhoid Fever' in the Han Dynasty and includes the addition of two herbs: *Panax ginseng* C.A.Mey. (Hongshen in Chinese) and Danshen (Hong et al., 2022). ESZWD suppresses myocardial fibrosis in chronic heart failure with heart-kidney yang deficiency (CHF-HKYD) (Hong et al., 2022). The CHF-HKYD rat model was established through intraperitoneal administration of combined thyroidectomy with DOX, which induces oxidative stress and subsequent myocardial fibrosis. ESZWD markedly attenuated myocardial fibrosis by reduction of collagen deposition and improvement of ventricular remodeling (restored heart weight-to-body weight ratio). ESZWD elevated LVEF and reduced LVIDd and LVIDs, which indicated the enhanced cardiac systolic function. ESZWD also decreased the serum levels of inflammatory cytokines, such as TNF-α, IL-11and IL-17A (Cheng et al., 2025).

The underlying mechanism of Danshen protecting against doxorubicin-induced cardiotoxicity

The normal mitochondrial integrity and function are essential for Ca^{2+} homeostasis and signaling transduction, as well as activation of the renin-angiotensin system (Ramalingam et al., 2017). DOX-induced cardiac toxicity is a multifactorial process in which overaccumulated oxidative stress plays a central role, and accumulated ROS stimulated lipid peroxidation (Vallejo et al., 2017), iron metabolism dysregulation, inflammation, ERS and mitochondrial permeability transition accompanied with loss of mitochondrial integrity and function. These pathological consequences contributed to the dose- and time-dependent cardiotoxicity of DOX and led to electrocardiographic irregularity, arrhythmias, cardiomyopathy and congestive heart failure which dramatically limit the clinical use of DOX in cancer patients (Pugazhendhi et al., 2018). We found that Danshen is potential for the treatment of DIC according to the previous studies. We systematically summarized the underlying molecular mechanism of Danshen and its ingredients protecting against DIC as below (Fig. 3).

Anti-apoptosis

PI3K/Akt/GSK-3β/JNK signaling pathway. The phosphatidylinositol 3-kinase/protein kinase B (PI3K)/Akt signaling pathway is the fundamental regulator of cell survival (Thapa et al., 2020; Vara et al., 2004). DOX significantly causes suppression of PI3K/Akt signaling by decreasing the phosphorylation of Akt, thereby initiating programmed cell death apoptosis in cardiomyocytes. Tan IIA, Tan I, Sal C and CPT ameliorated DIC through Akt activation (Chen et al., 2025; Ghanem et al., 2020; Hong et al., 2012; Jiang et al., 2022a; Wang et al., 2021a; Hong et al., 2012). Sal C and Tan IIA enhances Akt phosphorylation in a dose- and time-dependent manner, reduces apoptotic markers (cleaved caspase-3 and cytosolic cytochrome c), and upregulates the anti-apoptotic protein Bcl-xL in SD rat cardiomyocytes, H9c2 cells, HL-1 cells and C57BL/6 mice (Gao et al., 2008; Chen et al., 2025; Hong et al., 2012). The inhibition of PI3K or knockdown of Akt partially abolished Tan IIA's preventive effect from DIC-associated caspase-3 activation and apoptosis (Hong et al., 2012). CPT effectively attenuated DOX-induced ROS elevation, caspase activation and apoptosis via the activation of Akt-GSK-3β-mPTP signaling axis in cardiomyocytes (Wang et al., 2021a). CPT upregulates anti-apoptotic proteins including PI3K, p85, p-AKT, Bcl-2 and Bcl-xL, and increases phosphorylation of both Akt and glycogen synthase kinase-3β (GSK-3β). The phosphorylated GSK-3β disrupts the binding between adenine nucleotide translocase (ANT) and

cyclophilin D (CypD), thereby inhibiting mitochondrial permeability transition pore (mPTP) opening, preserving mitochondrial integrity and function and preventing the release of pro-apoptotic factors and subsequent caspase activation (Jacobs et al., 2012). Sal C enhances phosphorylation of PI3K (Tyr607), Akt (Ser473) and their downstream mTOR (Ser2448) while concurrently inhibits phosphorylation of JNK (Thr183/Tyr185) (Chen et al., 2025), which collectively reactivate the DOX-induced inhibition of cell survival pathways in cardiomyocyte. These results reveal that the activation of PI3K/Akt/GSK-3β is a central mechanism in Danshen and its active ingredients tanshinones protecting against DOX-induced cardiomyocyte apoptosis.

MAPKs signaling pathway. The mitogen-activated protein kinases (MAPKs) family, including extracellular signal-regulated kinase (ERK), c-Jun N-terminal kinase (JNK), p38/MAPK and ERK5, regulates a series of highly conserved enzymatic cascades, which are involved in a variety of physiological activities, in particular cell proliferation, differentiation and death (Cargnello and Roux, 2011). DOX causes significant activation of MAPKs signaling by upregulating the phosphorylation level of ERK and the level of JNK, leading to the initiation of apoptosis in cardiomyocytes (Zhang et al., 2016a). Mechanistic studies reveal that SMAE, CPT and DB exert potent anti-apoptotic effects in mitigating DIC through regulation of the MAPKs signaling pathway (Hung et al., 2020; Li et al., 2020; You et al., 2007; Yu et al., 2018a). SMAE suppressed cell apoptosis by inhibiting the ERK/p53 signaling cascade and decreasing the Bax/Bcl-xL ratio, cytochrome c release and caspase activation in H9c2 cells and male Wistar mice (Hung et al., 2020). CPT downregulates pro-apoptotic proteins, including 14-3-3σ, p-JNK, Bax, Bak, Bim, PUMA, and cleaved both caspases-9 and caspases-3 by inhibiting the p53 signaling pathway in H9c2 cells and male Wistar mice (Li et al., 2020). Additionally, CPT inhibited the nuclear translocation of p53 while promoting Foxo1 nuclear retention that further reinforced its anti-apoptotic effects in cardiomyocytes (Li et al., 2020; Wang et al., 2021a; Zhang et al., 2016b). DB exerts present anti-apoptotic effects against DIC primarily through modulation of the JNK signaling pathway (Yu et al., 2018a). DB promoted JNK1/2 activation and triggered downstream pro-survival pathways, potentially upregulating anti-apoptotic proteins and suppressing pro-apoptotic factors. And DB synergized with the AKT signaling to enhance mitochondrial protection and suppress ROS-mediated apoptosis (Yu et al., 2018a).

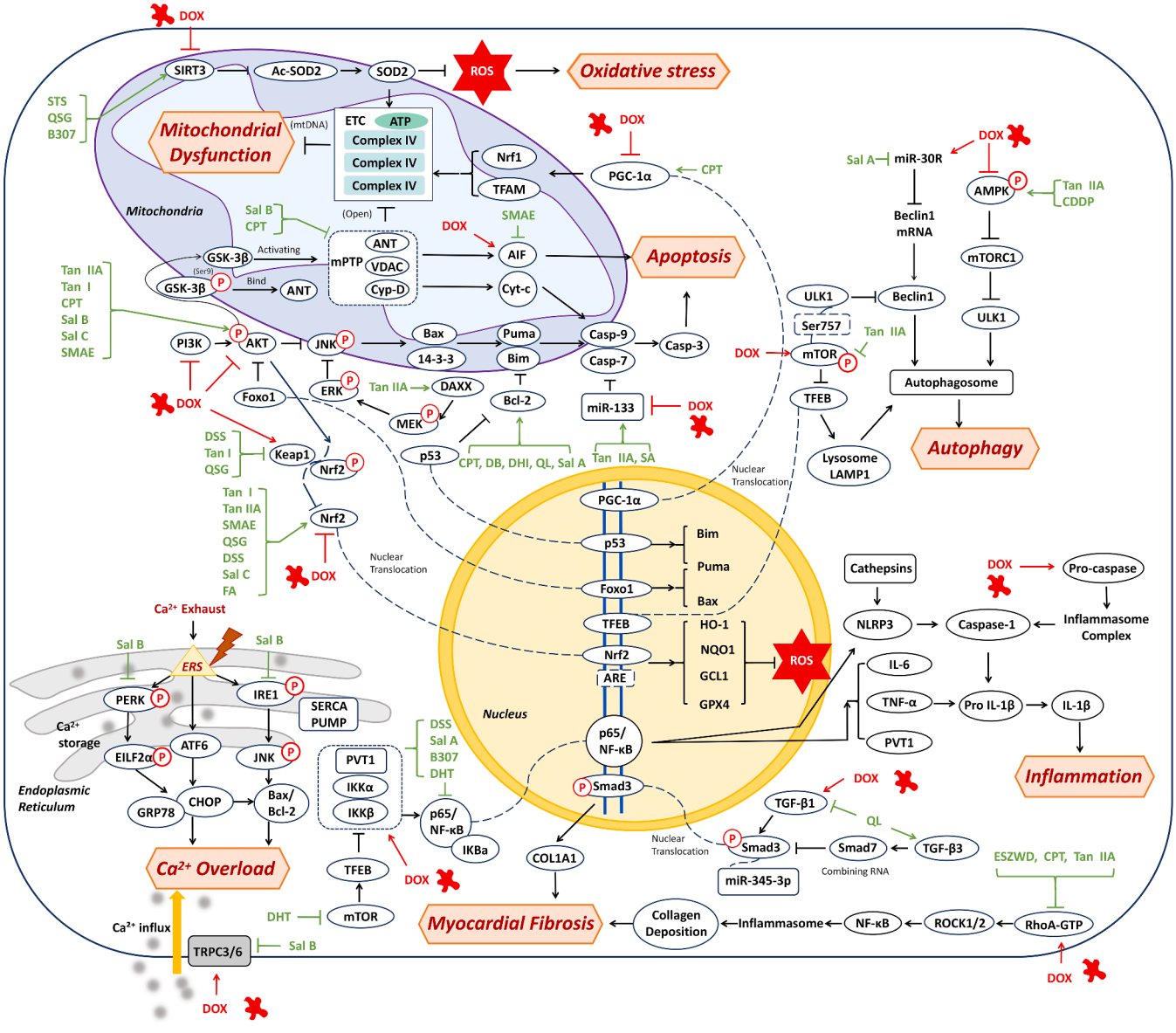

Fig. 3. Schematic overview of the potential underlying mechanisms related to the anti-DIC effect of *S. miltiorrhiza*.

Death-domain-associated protein (DAXX) serves as an upstream regulator of the MAPK signalling cascade. RNA-seq analysis revealed that Tan IIA significantly upregulated DAXX expression in H9c2 and HL-1 cardiomyoblasts. siRNA-targeted silencing completely abolished the effect of Tan IIA protecting against DIC. which confirmed the essential role of DAXX in Tan IIA's cardioprotective effect. Moreover, Tan IIA promoted the phosphorylation of mitogen-activated protein kinase (MEK) and its downstream target ERK1/2 in a DAXX-dependent manner, as shown by increased levels of p-MEK and p-ERK1/2, thereby activating the ERK1/2-mediated pro-survival signalling cascade (Xu et al., 2022a)

Overall, MAPKs are crucial in coordinating cellular responses to external environmental cues, and MAPKs signaling plays a central role in SMAE, CPT, Tan IIA and DB protecting against DIC.

Bax/Bcl-xL/Caspases signaling pathway. MiR-133 was identified as a direct inhibitor of caspase-9, which is a crucial initiator of the intrinsic apoptotic cascade (Feng et al., 2013; Song et al., 2017). Tan IIA significantly attenuated DOX-induced apoptosis in rat cardiomyoblast H9c2 by modulating the miR-133/caspase-9 signaling axis (Song et al., 2017). Tan IIA suppressed DOX-induced activation of caspase-9 and its downstream effectors including cleaved caspase-3 and poly (ADP-ribose) polymerase (PARP) by upregulation of miR-133 expression (Song et al., 2017). These findings elucidate a novel mechanism of Tan IIA protecting against DIC. DOX treatment significantly reduced the cell viability and induced apoptosis, increased pro-apoptotic proteins (Bax, cleaved caspase-3/9), and decreased anti-apoptotic Bcl-2 expression. Co-treatment of Sal A with DOX effectively reversed these effects by restoring cell viability, reducing apoptosis, and normalizing Bcl-2/Bax ratios (Wu et al., 2021).

In summary, Akt, caspases and MAPKs signaling might be the key targets for the anti-apoptosis effects of Danshen against DIC, in particular its lipophilic ingredients, with coordinated modulation.

Anti-oxidant

Keap1-Nrf2/NQO1 signaling pathway. The Keap1-Nrf2/NQO1 signaling pathway is a key cellular defense mechanism against oxidative stress (Aghagolzadeh et al., 2017). Kelch-like ECH-associated protein 1 (Keap1) acts as a cytoplasmic repressor of nuclear factor erythroid 2-related factor 2 (Nrf2) and leads Nrf2 for proteasomal degradation under basal conditions (Bellezza et al., 2018). NAD(P)H quinone oxidoreductase 1 (NQO1), a key Nrf2-regulated gene, plays a critical role in maintaining redox homeostasis by detoxifying reactive quinones and neutralizing free radicals (Ross and Siegel, 2021). Typically, Keap1 negatively regulates Nrf2 activity through ubiquitination; however, oxidative stress disrupts the Keap1-Nrf2 complex, liberating and activating Nrf2. Consequently, activated Nrf2 upregulates antioxidant genes, including NQO1 and heme oxygenase (HO-1), to mitigate oxidative damage (Zhang et al., 2021a). DOX induced elevation of Keap1 and reduction of Nrf2 and its downstream effectors NQO1 and HO-1, which was due to the exacerbated intracellular oxidative stress (Zhang et al., 2021a). Jia-ying et al. demonstrated that pretreatment of DSS dose-dependently reversed DOX-induced Keap1 upregulation and restores Nrf2/NQO1/HO-1 expression, thereby attenuating oxidative injury (Qi et al., 2022). QSG counteracted DOX-induced oxidative stress by reducing ROS, MDA and free iron accumulation, and restored intracellular glutathione (GSH) levels (Zhang et al., 2024). Mechanistically, QSG activated Nrf2 and promoted its nuclear translocation, which upregulated downstream antioxidant and iron-regulating proteins, including Glutathione Peroxidase 4 (GPX4), Ferritin Heavy Chain 1 (FTH1), Ferritin Mitochondrial (FTMT) and Ferroportin (FPN) (Xue et al., 2024). Tan I and Sal C similarly alleviated oxidative stress markers, including ROS, MDA and GSH, via activation of AKT/Nrf2 signaling pathway in both C57BL/6 mice and rat cardiomyoblast H9c2 (Chen et al., 2025; Jiang et al., 2022a; Jiang et al., 2022b). Tan I, Tan IIA, DSS, Sal C, CDDP and SMAE dose-dependently elevated total and nuclear Nrf2 protein levels and upregulated mRNA expression of Nrf2 and its downstream antioxidant genes like HO-1, NQO1, glutamate-cysteine ligase catalytic subunit (GCLC) in the heart of DOX-treated C57BL/6 and KM mice and H9c2 cells (Feng et al., 2021; Hung et al., 2020; Jiang et al., 2022a; Chen et al., 2025; Jiang et al., 2022b; Qi et al., 2022). siRNA-mediated Nrf2 knockdown reversed the protective effects of Tan IIA against DOX-induced cardiac toxicity (Guo et al., 2018). Additionally, the Danshen contained herbal formula B307, reduced ROS and 3-nitrotyrosine (3-NT) while increasing SOD2 in the heart of ICR mice (Lien et al., 2015), which might be correlated with activation of Nrf2 signaling. These findings collectively elucidate the crucial role of the Nrf2 signaling pathway in mediating the cardioprotective effects of Danshen and its constituents, including Tan I and Tan IIA, against DIC, and highlight their potential as adjuvant therapies in cancer treatment.

Scavenging of ASFR and lipid peroxidants. The adriamycin semiquinone free radical (ASFR), which is a reactive intermediate formed during the one-electron reduction of DOX by enzymes such as NADH dehydrogenase or xanthine oxidase, serves as a central mediator of DOX-induced cardiotoxicity (Davies and Doroshow, 1986; Nohl and Jordan, 1983). ASFR accumulates due to impaired redox cycling under anaerobic conditions, whereas it reacts with oxygen to generate superoxide anions (O_2^-) and hydroxyl radicals (-OH) in aerobic environments, initiating mitochondrial membrane lipid peroxidation. This process disrupts membrane integrity, promotes mitochondrial swelling, and inactivates membrane-bound enzymes, ultimately driving cardiac dysfunction (Griffin-Green et al., 1988; Ogura et al., 1991; Rajagopalan et al., 1988). STS counteracted these detrimental effects through dual mechanisms (Zhou et al., 2002): (1) STS rapidly oxidizes ASFR back to the quinone form of DOX under anaerobic conditions, thereby suppressing ASFR accumulation; (2) STS scavenges lipid radicals that are generated during lipid peroxidation, halting oxidative chain reactions, and significantly reduces mitochondrial swelling and hallmark of lipid peroxidation. *In vivo* studies further demonstrate that STS pretreatment mitigated endogenous lipid peroxidation in the hearts of DOX-exposed SD rats. Collectively, STS protected against DOX-induced oxidative stress by modulating ASFR redox dynamics and neutralizing lipid radicals, underscoring its potential as an adjuvant therapy for DIC.

SIRT3/Ac-SOD2 signaling pathway. The sirtuin 3 (SIRT3)/ acetylated superoxide dismutase 2 (Ac-SOD2) axis is a critical regulator of mitochondrial redox homeostasis and functional integrity. SIRT3, a mitochondrial NAD^+-dependent deacetylase, modulates oxidative stress resistance by deacetylating and activating key antioxidant enzymes, including SOD2. Deacetylation of SOD2 enhances its activity and ability to neutralize ROS in the mitochondria (Wu et al., 2022). DOX treatment suppressed SIRT3 expression, which elevated Ac-SOD2 levels and impaired SOD2 activity, consequently exacerbating ROS accumulation and mitochondrial dysfunction (Du et al., 2017). QSG administration mitigated DOX-induced oxidative stress and mitochondrial dysfunction and counteracted these deleterious effects by upregulating SIRT3 expression, reducing Ac-SOD2 levels, and increasing SOD2 activity (Zhang et al., 2024). These findings propose that SIRT3 activation might be a key mechanism for the antioxidant activity of *S. miltiorrhiza* in DIC.

In summary, the Keap1-Nrf2/NQO1 axis, ASFR scavenge and SIRT3/Ac-SOD2 signaling present pivotal roles in Danshen protecting against oxidative stress in DIC.

Anti-inflammation

NF-κB signaling pathway. The nuclear factor kappa B (NF-κB) signaling pathway serves a central role in DOX-induced inflammatory responses and apoptosis in cardiomyocytes (Lopez de Vergara et al., 2014). DOX

activated NF-κB through phosphorylation of IκB kinase (IKK) complex components (IKKα/β), which led to IκBα degradation and subsequent nuclear translocation of the p65 subunit of NF-κB. Activation of this signaling cascade upregulated pro-inflammatory cytokines TNF-α and IL-6 (Xu et al., 2020; Zhang et al., 2016a). Sal A presented potent anti-inflammatory and anti-apoptotic effects in the context of DIC by inhibiting the NF-κB signaling pathway (Oh et al., 2011; Wu et al., 2021). Furthermore, Sal A attenuated the expression of human plasmacytoma variant translocation 1 (PVT1), which is a long non-coding RNA that is implicated in exacerbating DOX-induced H9c2 cardiomyoblasts apoptosis and is upregulated by NF-κB activation. Sal A significantly mitigated the inflammation cascade and subsequent cellular damage by interfering with this DOX-NF-κB1-PVT1-apoptosis axis. DOX upregulated NF-κB expression at both mRNA and protein levels along with its downstream pro-apoptotic target lncRNA PVT1. Sal A suppressed DOX-induced NF-κB activation and PVT1 overexpression (Wu et al., 2021). DHT impeded inflammation by reducing nuclear translocation and activation of NF-κB in both H9c2 cardiomyoblasts and macrophages, consequently diminishing downstream inflammatory cytokines (TNF-α, IL-8 and COX2) levels (Imam et al., 2018; Wang et al., 2020a). The underlying mechanism was involved in the suppression of phosphorylation of mTOR and its downstream target S6K (Liu et al., 2015; Sahan-Firat et al., 2018), which facilitated the nuclear localization and expression of transcription factor EB (TFEB) and in turn hindered NF-κB activation by suppressing IKK phosphorylation (Brady et al., 2018). Thus, DHT orchestrated inflammation regulation through an mTOR-TFEB-IKK-NF-κB axis (Wang et al., 2020a). Furthermore, the herbal formula B307 presents similar anti-inflammatory effects by reducing NF-κB and TNF-α levels (Lien et al., 2015).

Taken together, the underlying mechanism of Danshen preventing DOX-induced cardiac inflammation is correlated with inhibition of the NF-κB signaling cascade.

Anti-cardiac fibrosis

TGF-β/Smads signaling pathway. The transforming growth factor-beta (TGF-β)/Smads signaling pathway is a pivotal regulator of cardiac fibrosis (Chen et al., 2018). TGF-β1, a dominant profibrotic isoform, binds to its receptor and activates Smad2/3, translocates into the nucleus and results in collagen synthesis and inflammatory cytokine release. Conversely, TGF-β3 antagonizes fibrotic responses by inducing the expression of Smad7, which is a negative regulator of cardiac fibrosis that blocks Smad3 phosphorylation and terminates TGF-β1 signaling (Deng et al., 2017). TGF-β1 and TGF-β3 maintain a dynamic balance under physiological conditions. However, DOX upregulated TGF-β1/Smad3 and suppressed TGF-β3/Smad7 signaling, consequently leading to extracellular matrix remodeling and myocardial dysfunction. QL presented significant cardioprotective effects against DOX-induced cardiac fibrosis through modulation of the TGF-β signaling pathway and antifibrotic microRNAs (Sun et al., 2020). QL inhibited the profibrotic TGF-β1 expression and Smad3 phosphorylation while simultaneously elevated the antifibrotic TGF-β3 and Smad7 levels. Crucially, QL upregulated the expression of miR-345-3p, which directly targeted the 3'-UTR of Smad3 mRNA and suppressed its translation according to the results from the luciferase reporter assay in HEK293 cells. This miRNA-mediated Smad3 silencing synergized with TGF-β3/Smad7 activation, which amplified the antifibrotic effect of QL. Notably, reduced nuclear translocation of Smad3 and enhanced Smad7 expression were consistently observed in QL-treated H9c2 cardiomyoblasts, which also provided direct evidence of TGF-β/Smad pathway modulation (Sun et al., 2020).

RhoA/ROCK signaling pathway. The ras homolog family member A/Rho-associated coiled-coil kinases (RhoA/ROCK) signaling pathway serves as a central regulator of fibroblast activation and cardiac remodeling in DIC (Xu et al., 2022b). RhoA, a small GTPase, initiates fibrosis by binding GTP and activating downstream effectors ROCK1/2, which phosphorylate LIM kinase and myosin light chain to drive cytoskeletal reorganization and α-SMA expression (Li et al., 2024b; Lu et al., 2024; Shimizu and Liao, 2016;). ROCK1/2 further promote collagen I A1 (COL1A1) synthesis through Smad3 phosphorylation and NF-κB-mediated inflammatory cytokine release (Lu et al., 2024). DOX activated RhoA, upregulated ROCK1/2 expression and led to cardiac fibroblast differentiation into myofibroblasts by upregulating α-SMA expression and increasing COL1A1 deposition, thereby driving pathological ventricular remodeling (Ge et al., 2025; Xu et al., 2022b). In DOX-treated SD rats, ESZWD significantly downregulated RhoA, ROCK1 and ROCK2 expression at both mRNA and protein levels, which suppressed RhoA/ROCK signaling activation, reduced collagen accumulation and improved cardiac function (Cheng et al., 2025). The antifibrotic effect of ESZWD was attributed to its bioactive components including Tan IIA and CPT, which can inhibit RhoA-GTP binding. These findings highlight that ESZWD alleviates DOX-driven myocardial fibrosis by disrupting RhoA/ROCK-mediated fibroblast activation and extracellular matrix overproduction, which also offers a mechanistic basis for its cardioprotective effects in CHF-HKYD.

In summary, the TGF-β/Smads and RhoA/ROCK signaling pathways present pivotal roles in Danshen's protection against cardiac fibrosis in DIC.

Anti-mitochondrial dysfunction

Akt-GSK-3β-mPTP signaling pathway. The Akt-GSK-3β-mPTP signaling axis plays a pivotal role in DOX-induced mitochondrial dysfunction (Wang et al., 2021a). Akt phosphorylates and inactivates GSK-3β at serine 9 (Ser9), thereby suppressing its capacity to promote mPTP opening through interaction with ANT and CypD (Wang et al., 2013). DOX disrupts mitochondrial membrane integrity by inhibiting Akt phosphorylation and activation, subsequently leading to GSK-3β activation and subsequent stabilization of the CypD-ANT complex, which triggers mPTP opening (Wang et al., 2021a). CPT counteracted this process by enhancing Akt phosphorylation, which induced the inhibitory phosphorylation of GSK-3β at Ser9 and suppressed its binding to ANT while disrupting the CypD-ANT complex formation and stabilizing mPTP closure. This regulatory mechanism preserved mitochondrial membrane potential, reduced ROS accumulation and suppressed caspase-dependent apoptotic pathways. By modulating the Akt-GSK-3β cascade, CPT effectively maintained mitochondrial homeostasis and attenuated mPTP-driven H9c2 cardiomyoblast death, highlighting its therapeutic potential in alleviating DIC.

PGC-1α/NRF-1/TFAM signaling pathways. Mitochondrial dysfunction contributes to the pathogenesis of DIC, which is characterized by impaired biogenesis, disrupted electron transport chain (ETC) activity, and exacerbated oxidative stress (Sun et al., 2013). Peroxisome proliferator-activated receptor-γ coactivator 1-α (PGC-1α) acts as a transcriptional coactivator that binds to nuclear receptors including ERRα and PPARγ to initiate mitochondrial biogenesis, followed by stimulating the expression of nuclear-encoded mitochondrial genes that are involved in oxidative phosphorylation (Chowanadisai et al., 2010). DOX suppressed PGC-1α expression, thereby halting mitochondrial DNA (mtDNA) replication and new organelle synthesis. Nuclear respiratory factor 1 (NRF-1) directly binds to the promoters of genes encoding ETC complexes and mitochondrial transcription machinery, facilitating nuclear-mitochondrial crosstalk (Scarpulla, 2002). DOX downregulated NRF-1 expression, which impaired the transcription of ETC components such as Complex IV subunits (Zhang et al., 2016b). Mitochondrial Transcription Factor A (TFAM) binds to mtDNA to stabilize its structure, promote replication, and regulate transcription of mtDNA-encoded ETC subunits. DOX reduced the TFAM expression level, which led to mtDNA

depletion and impaired synthesis of critical ETC proteins. CPT demonstrated protective effects against DIC by maintaining mitochondrial function and promoting mitochondrial biogenesis (Wang et al., 2021a; Zhang et al., 2016b) and the underlying molecular mechanism was related to the upregulation of DOX-suppressed key regulators of mitochondrial biogenesis including PGC-1α, NRF-1 and TFAM (Chowanadisai et al., 2010).

ATP production is the primary function of mitochondria. Four membrane-bound ETCs (complex I, II, III, and IV) that are embedded in the inner membrane have been identified as critical factors in ATP production since their activities determine the ATP generation rate (Kadenbach et al., 2011; Sun et al., 2013). DOX reduced the mitochondrial membrane potential (MMP), which is vital for maintaining the proton gradient necessary for ATP synthesis via oxidative phosphorylation, and impaired the activity of ETC, in particular complexes I, III and IV, while complex II remained unaffected (Zhao et al., 2019). CPT partially restored DOX-induced reduction of MMP and the dysfunction of electron transportation by restoring ATP synthesis and enhancing MMP through protection of complexes I, III and IV (Zhang et al., 2016b). Furthermore, CPT significantly downregulated superoxide anion free radical production, which further attenuated oxidative stress and protected mitochondrial ATP synthesis (Kadenbach et al., 2011; Sun et al., 2013; Zhang et al., 2016b).

Nrf2-GPX4 signaling pathway. Apart from directly targeting mitochondria, *S. miltiorrhiza* derivatives mitigated DIC-associated mitochondrial dysfunction through extrinsic regulatory networks involving calcium homeostasis modulation, inter-organelle ROS crosstalk and ferroptosis suppression. CPT and Tan IIA synergistically protected mitochondrial integrity through multiple pathways (Wang et al., 2021a; Zhang et al., 2010). CPT stabilized the mitochondrial outer membrane integrity by enhancing the expression of anti-apoptotic proteins (Bcl-2) and suppressing pro-apoptotic factors (cleaved caspase 3/7 and Bax). CPT prevented ROS-mediated mitochondrial damage by reducing superoxide production and elevating GSH-Px activity (Zhang et al., 2016b). Tan IIA complemented these effects by downregulating caspase-3/8 and improving MMP to reinforce apoptosis resistance (Li et al., 2020). In addition, Sal B inhibited transient receptor potential canonical (TRPC) 3/6-mediated calcium overload, indirectly preventing ERS-induced mitochondrial apoptosis and inhibiting caspase-12 activation, which also stabilized the integrity of mitochondrial membrane (Chen et al., 2017). QSG upregulated the mitochondria residential level of SIRT3 which enhanced SOD2 activity, improved ATP synthesis, reduced ROS and restored mitochondrial redox balance (Zhang et al., 2024). DHT counteracted DOX-induced mitochondrial depletion by activation of TFEB, which is a master regulator of lysosomal and mitochondrial biogenesis (Wang et al., 2020a). DOX depleted mitochondrial GSH and promoted iron accumulation, thereby leading to cardiolipin peroxidation and ETC disruption (Tadokoro et al., 2020). Both FA and DSS restored mitochondrial GSH levels and reduced lipid peroxides on the mitochondrial membranes via activation of the Nrf2-GPX4 axis. DSS eliminated DOX-induced accumulation of mitochondrial ROS and intracellular heme and suppressed iron overload by upregulating HO-1/NQO1 levels (Qi et al., 2022).

Mitochondrial integrity. Apoptosis-inducing factor (AIF) is a flavoprotein essential for oxidative phosphorylation that triggers caspase-independent apoptosis when it is released into the cytoplasm (Rao et al., 2019). DOX compromised mitochondrial integrity through permeability transition pore opening, which caused nuclear translocation of AIF. DOX also activated lysosomal cathepsin B, which is a lysosomal cysteine protease that mediates autophagic flux impairment and executes apoptosis via Bid cleavage, and was involved in the degradation of proteins and organelles, antigen presentation and execution of cell death pathways (Xie et al., 2023). SMAE stabilized lysosomal membranes and inhibited cathepsin B leakage (Hung et al., 2020). CPT and SMAE prevented AIF nuclear translocation by preserving mitochondrial integrity (Hung et al., 2020; Wang et al., 2021a; Zhang et al., 2016b). The coordinated suppression of lysosomal-mitochondrial crosstalk effectively attenuated DOX-driven cardiomyocyte death.

In summary, the Akt-GSK-3β-mPTP axis, PGC-1α/NRF-1/TFAM transcriptional network and SIRT3/ETC-Bcl-2/GPX4 signaling represent pivotal roles of Danshen's protection against mitochondrial dysfunction in DIC.

Blockage of Ca^{2+} channels and ERS

Disruption of intracellular calcium homeostasis is one of the hallmarks in DIC. The TRPC ion channels, in particular TRPC3 and TRPC6, function as essential mediators of calcium influx in cardiomyocytes (Nishiyama et al., 2021; Tai et al., 2017). DOX resulted in pathological Ca^{2+} overload by significantly upregulating the expression of TRPC3 and TRPC6. The excessive intracellular Ca^{2+} accumulation disturbs cardiac homeostasis and triggers ERS, which may ultimately initiate the unfolded protein response (UPR) (Senft and Ronai, 2015). When the UPR activation is excessive and prolonged, it results in cell apoptosis through three main ERS sensors including PKR-like ER kinase (PERK), inositol-requiring enzyme 1 (IRE1) and activating transcription factor-6 (ATF-6) (Bahar et al., 2016; Yang et al., 2015). Sal B effectively reduced DOX-induced ERS by suppressing PERK, IRE1 and ATF-6 in DOX-treated cardiomyocytes, thereby preventing the activation of downstream apoptotic cascades. Sal B inhibited DOX-triggered TRPC3/6 overexpression, which normalized intracellular Ca^{2+} levels. Pretreatment with Sal B attenuated ERS by suppressing DOX-induced elevated expression of CHOP and GRP78, which are two biomarkers of ERS (Chen et al., 2017). Notably, Sal B exhibits remarkable cardioprotective effects against DOX-induced cardiac dysfunction through modulation of both Ca^{2+} homeostasis and ERS-related pathways.

The PI3K/Akt signaling pathway is a critical regulator of ERS and Ca^{2+} homeostasis in cardiomyocytes. PI3K activation induces Akt phosphorylation, which modulates ER Ca^{2+}-ATPase (SERCA) activity and stabilizes ER function under stress conditions (Viskupicova and Rezbarikova, 2022). DOX led to ER Ca^{2+} dysregulation, activation of ERS sensors (IRE1, PERK and ATF6) (Ron and Walter, 2007) and subsequent apoptosis via reduction of Akt and GSK-3β phosphorylation and suppression of PI3K/Akt signaling. In physiological conditions, phosphorylated Akt inhibits ERS by maintaining Ca^{2+} homeostasis (Dong et al., 2013). However, DOX disrupted this protective mechanism by suppressing Akt phosphorylation (Mao et al., 2008), consequently causing ER Ca^{2+} leakage, upregulation of GRP78 and CHOP, and initiation of apoptotic cascades (Ron and Walter, 2007; Sishi et al., 2013). Sal B prevented DOX-induced cardiotoxicity by enhancing phosphorylation of Akt and GSK-3β, which stabilizes ER Ca^{2+} stores and suppresses ERS. In addition, Sal B alleviated DOX-induced ERS by reducing intracellular Ca^{2+} levels and suppressing the protein levels of GRP78, CHOP and ERS transducers (p-IRE1, p-PERK and ATF6) (Chen et al., 2016).

In summary, the TRPC3/6/Ca^{2+} and PI3K/Akt signaling pathways present pivotal roles in Danshen suppressing Ca^{2+} overload and ERS in DIC.

Regulation of autophagy

miR-30a/Beclin1/LAMP1 signaling pathway. MicroRNAs (miRNAs) are intimately associated with various cardiac functions, including cell development, electrical signaling and myocardial contraction (Dill and Naya, 2018; Fa et al., 2021). Beclin1, which is an evolutionarily conserved eukaryotic protein, is indispensable for autophagosome nucleation and maturation and acts as a core constituent of the class III PI3K complex (Chang et al., 2019). The miR-30a/beclin1 signaling pathway served as a crucial regulatory mechanism in DIC (Chang et al.,

2019; Roca-Alonso et al., 2015; Zhang et al., 2021b). DOX administration significantly upregulated miR-30a expression in zebrafish, which suppressed Beclin1-dependent autophagosome-lysosome fusion (Li et al., 2024a). SA reduced autophagosome retention, improved lysosomal degradation and mitigated DOX-induced H9c2 cardiomyoblast apoptosis by downregulating miR-30a expression and restoring Beclin1-mediated autophagic flux (Li et al., 2024a). These findings highlight SA's therapeutic potential via inhibition of miR-30a/beclin1-dependent autophagy in DIC.

The Beclin1/Lysosomal-associated membrane protein 1 (LAMP1) signaling pathway serves as a central regulator of autophagy, which is a critical cellular process for maintaining cardiac myocardial homeostasis (Bartlett et al., 2017; Li et al., 2016b; Orogo and Gustafsson, 2015). Beclin1 facilitates autophagosome formation while LAMP1 ensures lysosomal integrity and autolysosome degradation (Gurkar et al., 2013; Zhou et al., 2013). Under physiological conditions, mTOR suppresses autophagy through phosphorylation of unc-51-like autophagy-activating kinase 1 (ULK1) at Ser757, thereby inhibiting its kinase activity and autophagosome initiation (Orogo and Gustafsson, 2015; Zhou et al., 2013). Concurrently, mTOR-mediated phosphorylation of TFEB-induced cytoplasmic sequestration and prevents nuclear translocation of the transcription factor, followed by downregulating lysosome biogenesis genes including LAMP1. DOX impaired autophagic flux via mTOR hyperactivation, which suppressed ULK1-Beclin1-dependent autophagosome biogenesis. In the meantime, DOX caused lysosomal dysfunction which was manifested by diminishing acidification capacity and impairing cathepsin B activity, ultimately resulting in autophagosome accumulation (Bartlett et al., 2016; Li et al., 2016b). Tan IIA exerted dual regulatory effects on promoting autophagy, followed by inhibiting mTOR activity (Wang et al., 2019a). First, Tan IIA activated Beclin1-dependent autophagosome formation by reducing the inhibitory phosphorylation of ULK1. Second, Tan IIA facilitated TFEB nuclear translocation which augmented LAMP1-mediated lysosomal functionality. These findings demonstrate that Tan IIA regulates autophagic processes via regulation of the Beclin1/LAMP1 pathway, which promotes the formation of autophagosomes and effectively restores the DOX-disrupted imbalance of autophagic flux.

AMPK signaling pathway. AMP-activated protein kinase (AMPK), a central cellular energy sensor, regulates autophagy by modulating downstream targets including mTOR (Hardie, 2003). DOX typically inhibited AMPK phosphorylation, impairing its regulatory function in energy homeostasis (Timm and Tyler, 2020). Tan IIA and CDDP pharmacologically rescues this pathological state by restoring AMPK phosphorylation (Feng et al., 2021; Wang et al., 2019b). Activated AMPK exerts inhibitory control over the mechanistic target of rapamycin complex 1 (mTORC1), consequently ablating mTORC1-mediated suppression on ULK1 and initiating autophagosome formation (Mihaylova and Shaw, 2011; Zhang et al., 2023). In cardiomyocytes H9c2, Tan IIA enhanced autophagic flux, which is a crucial process for maintaining cellular homeostasis and alleviating oxidative stress by activating the AMPK signaling pathway, consequently ameliorating cellular damage in DIC (Yuan et al., 2019a).

In summary, the miR-30a/Beclin1/LAMP1 axis and AMPK signaling pathway are important for Danshen derivatives protecting against DOX-induced autophagic dysfunction in DIC.

Clinical trials related to Danshen treating cardiovascular and cerebrovascular diseases

Danshen and its derivatives are widely used in traditional Chinese medicine while there is still a lack of clinical trials related to evaluation their efficacy in DIC. The current modern clinical research mainly focus on their treatment effects for cardiovascular and cerebrovascular diseases (Ren et al., 2019). All the Danshen-related clinical trials in cardiovascular and cerebrovascular diseases are summarized in Table 3, which covers interventions, registration numbers, conditions, locations, statuses, phases and results. The data were retrieved from the Chinese Clinical Trial Registry (ChiCTR, https://www.chictr.org.cn/indexEN.html) and International Traditional Medicine Clinical Trial Registration Platform (ITMCTR, http://itmctr.ccebtcm.org.cn/) on 20 May 2025. Most of the clinical research on Danshen focused on its use as an adjuvant therapy for cardiovascular and cerebrovascular diseases. For coronary heart disease (CHD), multiple trials investigate Danshen-based interventions (CDDP and SA injection) for conditions like chronic stable angina (ChiCTR2400093487), acute anterior wall myocardial infarction (ITMCTR2025000365) and post-percutaneous coronary intervention (PCI) angina pectoris (ITMCTR2200005650). In the context of cerebrovascular diseases, studies primarily focus on acute ischemic stroke (ChiCTR2200055219) and its convalescence phase (ITMCTR1900002623), which evaluate neuroprotective and microcirculation-improving effects of Danshen-based treatment. Notably, several trials address diabetic cardiovascular complications, such as impaired coronary microcirculation in diabetic patients (ITMCTR2200005813), while others explore its role in carotid plaque management (ITMCTR2025000263, ITMCTR2025000264). For psychosomatic comorbidities in CVDs, a few studies examine the impact of Danshen on depression and anxiety post-PCI (ChiCTR1900023457, ITMCTR1900002368).

Overall, the majority of trials are concentrated in cardiovascular and cerebrovascular indications, with a growing but smaller body of research in cardiovascular disease-related neuronal (mental) disorders and metabolic disorder-associated cardiovascular complications.

Discussion

This systematic review critically evaluates the protective effects of *S. miltiorrhiza* (Danshen) and its associated ingredients, derivatives, extracts and formulas against DIC. The findings from both *in vitro* and *in vivo* studies consistently demonstrate that Danshen exerts significant cardioprotective effects through multiple mechanisms including anti-apoptosis, anti-inflammation, anti-oxidative stress, anti-fibrosis, induction of autophagy and maintenance of calcium homeostasis, mitochondrial function and mitochondrial integrity etc.. These protective effects are mediated through the modulation of key signaling pathways including ERK/p53, JNK1/2, PI3K/Akt and Akt-GSK-3β-mPTP signaling pathways etc.. But currently Danshen-related clinical trials mainly focus on the treatment of cardiovascular and cerebrovascular diseases according to the data extracted from clinical register databases. There is a lack of clinical trials for the evaluating the efficacy of Danshen-related agents for treatment of DIC although all these *in vivo* and *in vitro* findings highlight the potential value of Danshen in preventing or treating DIC.

Whether Danshen protects against DIC, in the meantime, not affecting the anticancer efficacy of DOX is the most important issue that should be considered in a translational insight. Danshen contains two major bioactive ingredient groups including lipophilic tanshinones and hydrophilic phenolic acids, which demonstrate both cardioprotective and anticancer properties (Chen et al., 2014). CPT exerted direct antitumor effects by elevating intracellular ROS, suppressing MAPK-AKT signaling and inhibiting proliferation in gastric and lung cancer cells, while concurrently protecting H9c2 cardiomyoblasts through mPTP

Table 3
The summary of clinical trials of Danshen-based interventions in cardiovascular and cerebrovascular diseases.

Intervention/ treatment	Registration number	Condition	Location	Type	Status	Phase	Results
Coronary Artery Disease (CAD) and Angina							
Tan IIA dissolving acupoint microneedles	ChiCTR2400093487	Chronic stable angina	China/Guizhou/ Guiyang	Interventional study	Recruiting	Phase 0	Not mentioned
Oral Danlou tablets + intravenous Salvia miltiorrhiza ligustrazine injection	ChiCTR1900025601	Chronic Stable Angina	China/ Heilongjiang	Observational study	Completed	Not Applicable	Not mentioned
Danshen injection	ChiCTR1900021590	Stable CHD	China/ Guangdong	Interventional study	Prospective registration	Phase 4	Not mentioned
Intravenous salvianolate	ChiCTR1800018772	Stable coronary heart disease with high FFR (>0.8) and IMR (>25)	China/Zhejiang	Interventional study	Prospective registration	Phase 4	Not mentioned
Danshen dripping pills + Aspirin	ChiCTR-IPR-17012014	Stable exertional angina pectoris (TCM Blood Stasis Syndrome)	China/Tianjin	Interventional study	Prospective registration	Phase 4	Not mentioned
Experimental group: Guanxin Qiwei dropping pills; Control group: CDDP	ChiCTR-IPR-15006605	Stable angina pectoris with blood stasis syndrome (CAD)	China/Liaoning, Sichuan, Chongqing	Interventional study	Retrospective registration	Phase 4	Not mentioned
Improved CSDP vs. Original CSDP	ChiCTR-TRC-09000576	Stable angina pectoris (Qi stagnation blood stasis syndrome)	China/Tianjin	Interventional study	Completed	Phase 4	Not mentioned
Astragalus and Salvia miltiorrhiza drug pairs	ITMCTR2025000058	Stable Coronary artery disease	China/ Shandong/Jinan	Observational study (retrospective cohort)	Prospective registration	Retrospective study	Not mentioned
Conventional Western medicine treatment plus CDDP	ChiCTR2400080149	Coronary artery disease	China/ Guangdong/ Yangjiang	Interventional study	Completed	Phase 4	Not mentioned
Salvianolate injection; Aspirin + Salvianolate injection	ChiCTR2200063135	Coronary artery disease stable angina pectoris	China/Beijing	Interventional study	Prospective registration	Not Applicable	Not mentioned
Danshen Beverage + conventional Western medicine	ITMCTR2024000028	Coronary artery disease	China/ Guangdong/ Guangzhou	Interventional study	Retrospective registration	Not Applicable	Not mentioned
Salvianolate group: Salvianolate injection + standard therapy	ChiCTR-IPR-15005998	Coronary artery disease (non-ST elevation ACS or stable angina) undergoing angiography/intervention	China/Beijing	Interventional study	Prospective registration	Phase 4	Not mentioned
Treatment with Danshen Chuanxiong or Danshen Sanqi prescriptions	ITMCTR2025000478	Stable coronary atherosclerotic heart disease	China/ Shandong/Jinan	Observational study (retrospective cohort)	Prospective registration	Retrospective study	Not mentioned
CDDP	ChiCTR-TRC-14004327	Maintenance hemodialysis patients with coronary artery disease	China/ Guangdong	Interventional study	Completed	Phase 0	Not mentioned
Acute Coronary Syndrome (ACS) and Myocardial Infarction							
CDDP	ChiCTR2200060193	Acute anterior wall myocardial infarction	China/Jiangsu/ Xuzhou	Interventional study	Prospective registration	Phase 4	Not mentioned
CDDP	ChiCTR2000033262	Acute anterior wall myocardial infarction	China/Jiangsu/ Nanjing, Xuzhou, etc.	Interventional study	Prospective registration	Phase 4	Not mentioned
CDDP	ITMCTR2025000365	Acute ST-elevation myocardial infarction (STEMI)	China/Shanghai	Interventional study	Retrospective registration	Not Applicable	Not mentioned
Conventional treatment + CDDP	ITMCTR2000003341	Acute anterior ST-segment elevation myocardial infarction (STEMI)	China/Jiangsu (Multi-center)	Interventional study	Prospective registration	Phase 4	Not mentioned
Salvianolate injection	ChiCTR-IPR-17010501	Acute STEMI post-primary PCI	China/Shanghai	Interventional study	Prospective registration	Phase 4	Not mentioned
Salvianolate injection	ChiCTR-TRC-08000060	Acute ST-elevation myocardial infarction (STEMI) undergoing primary PCI	China/Shanghai (Multicenter)	Interventional study	Completed	Phase 4	Not mentioned
STS injection	ChiCTR1800020340	Acute coronary syndrome (ACS)	China/ Guangdong	Interventional study	Prospective registration	Phase 4	Not mentioned
Treatment group: STS + standard therapy	ChiCTR-TRC-14005182	Acute coronary syndrome (NST-ACS) undergoing PCI	China/ Guangdong, Shanghai, Beijing	Interventional study	Prospective registration	Phase 4	Not mentioned
STS + simvastatin	ChiCTR-TRC-12002361	CHD with unstable angina/ non-ST elevation MI	China/Beijing	Interventional study	Completed	Phase 4	Not mentioned
PCI Complications and Angina							
Basic treatment + FuFang DanShen Pian	ChiCTR2300068681	Heart failure after PCI in acute myocardial infarction	China/ Guangdong/	Interventional study	Prospective registration	Phase 4	Not mentioned

(*continued on next page*)

Table 3 (*continued*)

Intervention/ treatment	Registration number	Condition	Location	Type	Status	Phase	Results
			Guangzhou, Dongguan, Jiangmen				
Salvia tablets	ChiCTR2100047615	Post-PCI angina pectoris	China/Shanghai	Interventional study	Prospective registration	Phase 4	Not mentioned
CDDP	ChiCTR2000032384	Refractory angina with incomplete revascularization	China/ Guangdong/ Guangzhou	Interventional study	Prospective registration	Phase 4	Not mentioned
Intensive CDDP treatment vs. Standard	ChiCTR-IIR-17013662	Refractory angina in patients unsuitable for revascularization	China/ Guangdong/ Guangzhou	Interventional study	Prospective registration	Phase 4	Not mentioned
Intensive Treatment Group: CDDP 20 pills TID	ITMCTR2000003248	Refractory angina with incomplete revascularization	China/ Guangdong (Multi-center)	Interventional study	Prospective registration	Phase 4	Not mentioned
STS combined with hydration pretreatment	ChiCTR2300070064	Contrast-induced acute kidney injury in PCI	China/Henan/ Kaifeng	Interventional study	Prospective registration	Phase 4	Not mentioned
Conventional western medicine + Gualou Danshen Granules	ChiCTR2000031780	Unstable angina pectoris (phlegm-blood stasis syndrome)	China/Beijing	Interventional study	Prospective registration	Phase 2	Not mentioned
Salvianolate injection	ChiCTR-IPR-17010481	Unstable angina pectoris (elderly patients aged 60-85)	China/Beijing, Tianjin, Shanghai	Interventional study	Retrospective registration	Phase 4	Not mentioned
Conventional Western medicine + Gualou Danshen Granules	ITMCTR2000003201	Unstable angina pectoris with Phlegm-Blood Stasis Syndrome	China/Beijing	Interventional study	Prospective registration	Phase 2	Not mentioned
Carotid Plaque (Atherosclerosis)							
Danshen Sanqi Decoction	ITMCTR2025000264	Carotid plaque	China/ Shandong/Jinan	Observational study (retrospective cohort)	Prospective registration	Retrospective study	Not mentioned
Salvia and Ligusticum Formula	ITMCTR2025000263	Carotid plaque	China/ Shandong/Jinan	Observational study (retrospective cohort)	Prospective registration	Retrospective study	Not mentioned
Danshen Huangqi Decoction	ITMCTR2025000262	Carotid plaque	China/ Shandong/Jinan	Observational study (retrospective cohort)	Prospective registration	Retrospective study	Not mentioned
Diabetes and Cardiovascular Complications							
CDDP	ChiCTR2200058304	Impaired coronary microcirculation in diabetic patients	China/Shanghai	Interventional study	Prospective registration	Not Applicable	Not mentioned
CDDP	ITMCTR2200005813	Coronary microcirculation disorder in diabetic patients	China/Shanghai	Interventional study	Prospective registration	Not Applicable	Not mentioned
Standard therapy + Composite Danshen Pill	ChiCTR-IPR-15006501	Type 2 diabetes with cardiovascular disease or risk factors	China/Shanghai	Interventional study	Prospective registration	Phase 4	Not mentioned
Tan IIA + standard oral hypoglycemic therapy	ChiCTR-TQR-14005142	Early renal damage in type 2 diabetes (microalbuminuria)	China/Hebei	Quasi-randomized controlled trial	Prospective registration	Not Applicable	Not mentioned
Cerebrovascular Diseases							
SA for Injection	ChiCTR2200055219	Acute ischemic stroke	China/Tianjin, Henan, Hebei, etc.	Observational study	Prospective registration	Phase 4	Not mentioned
SA injection	ChiCTR1800015677	Large cerebral infarction	China/Shanxi/ Taiyuan	Interventional study	Prospective registration	Phase 4	Not mentioned
S. Miltiorrhizae Polyphenolic Acid Injection	ITMCTR1900002623	Ischemic stroke (convalescence)	China/Tianjin, Beijing, Anhui	Observational study (single-arm)	Recruiting	Post-marketing	Not mentioned
CAD-associated Mental Health Complications							
Taking Guanxin Danshen Dripping Pills	ChiCTR2100051523	Coronary artery disease combined with depression or anxiety	China/Shanghai	Observational study	Prospective registration	Phase 4	Not mentioned
Basic therapy + Guanxindanshen Dropping Pills	ChiCTR1900023457	Depression/anxiety post-PCI for CHD	China/Beijing, Shanghai, Guangdong, Jilin	Interventional study	Retrospective registration	Phase 4	Not mentioned
Guanxin Danshen Dropping Pills	ChiCTR1800014291	CHD post-PCI with anxiety/ depression	China/ Guangdong	Interventional study	Retrospective registration	Phase 4	Not mentioned
Basic therapy + Guanxindanshen Dropping Pills	ITMCTR1900002368	Post-PCI CHD with depression/anxiety	China/Beijing, Shanghai, etc.	Randomized controlled trial	Retrospective registration	Post-marketing	Not mentioned

blockade (Zheng et al., 2024). Tan I inhibited non-small cell lung cancer (CL1-5) invasion and metastasis by suppressing IL-8-mediated angiogenesis via AP-1/NF-κB blockade, while inducing apoptosis in breast cancer (MDA-MB-231) through Bcl-2 downregulation and caspase-3 activation (Lee et al., 2008; Nizamutdinova et al., 2008). Tan IIA mitigated DOX-induced cardiotoxicity via activation of Akt/ERK pathways while suppressing breast (MDA-MB-453), liver (HepG2) and lung (A549) cancer cell viability through induction of mitochondrial apoptosis and anti-angiogenesis (Chiu and Su, 2010; Xu and Xi, 2009; Yuan et al., 2004). Sal A inhibited nucleoside transport in Ehrlich carcinoma cells, which suppressed cancer cell proliferation and synergistically enhanced chemotherapy efficacy (Zhang et al., 2004). Sal B attenuated cardiac oxidative stress while combating squamous cell carcinoma via COX-2/VEGF inhibition (Hao et al., 2009). DHT inhibited cervical cancer progression by inducing microtubule disruption-mediated G_2/M cell cycle arrest (Ye et al., 2012), DSS suppressed melanoma metastasis (B16F10) and liver metastatic foci by blocking VEGF-driven migration (Yang et al., 2025). These results present a fundamental translational gap, and we explicitly emphasize that evaluating Danshen-DOX interactions must be a priority for future research.

Although this systematic review demonstrates the cardioprotective potential of Danshen and its active components against DIC, several limitations should be acknowledged. First, the heterogeneity among the studies in terms of experimental designs, dosages and outcome measures may limit the comparability and generalizability of the results according to the SYRCLE's tool that many of the studies suffer from a risk of bias. Most of the studies only mentioned "randomization" but did not introduce specific approaches. Mechanistic over reliance on correlative evidence weakens causal claims. Second, no study has established a therapeutic dosage window that balances cardioprotection with antitumor synergy and tissue safety, which is a major hurdle for clinical translation. Few studies directly addresses Danshen protecting against DIC without affecting anti-cancer efficacy of DOX under a certain cancer condition. Only one included study B307, which did not interfere with the cytotoxic activity of DOX in human Huh7 hepatoma cells and was non-cytotoxic itself. Third, no trial demonstrates that Danshen treatment improves cardiac function and reduces mortality in DOX-treated cancer patients. All the Danshen-associated clinical trials evaluate its effecacy in cardiovascular and cerebrovascular disorders, and these findings require cautious interpretation due to the overall low quality of current randomized controlled trials (RCTs). There is a need for standardized multicenter, randomized, double-blind and placebo-controlled trials that are designed following the CONSORT guidelines to validate these results. The current adressed clinical trials exhibit critical methodological limitations, including geographical restrictions (enrollment limited to Chinese cohorts), absence of data on chemotherapy interactions, in particular whether cardioprotection compromises DOX's antitumor efficacy, and omission of cancer-specific endpoints such as tumor progression and cardiac microenvironment remodeling under malignancy. Fourth, critical toxicities also lack comprehensive dose-exposure profiles and some compounds pose toxicological concerns. The reported cardiovascular benefits remain inconclusive due to the unaddressed risks of teratogenicity and tissue-specific toxicity. CPT exhibited tissue-specific toxicity with inhibiting fibroblast-like synoviocyte proliferation at 3 μM, which is a concentration lower than its cardioprotective threshold 10 μM in cardiomyocytes, and demonstrated teratogenic effects (pericardial edema and scoliosis) in zebrafish (Zheng et al., 2024). For CDDP, long-term organ toxicity, e.g. renal or immunological toxicity, and herb-drug interaction are remain uncharacterized (Luo et al., 2015). DSS presents translational challenges due to its chemical instability and low oral bioavailability (Xue-Jiao et al., 2017).

Conclusion

In conclusion, accumulated evidence supports the cardioprotective efficacy and safety of Danshen against DIC. Danshen exhibits a huge potential as a therapeutic agent for DIC and chemotherapy-related cardiovascular complications, although further clinical trial validation and evaluation of long-term outcomes are needed. The findings of this systematic review have important implications for future research and clinical practice of Danshen.

CRediT authorship contribution statement

Mei-Yan Yue: Writing – review & editing, Writing – original draft, Visualization, Methodology, Conceptualization. **Wai-Rong Zhao:** Validation, Resources, Project administration, Investigation, Funding acquisition. **Shan-Shan Wang:** Writing – original draft, Investigation, Formal analysis. **Jing Zhang:** Investigation, Formal analysis. **Wen-Ting Shi:** Investigation, Formal analysis. **Jing-Yi Tang:** Resources, Project administration, Methodology, Funding acquisition. **Zhong-Yan Zhou:** Writing – review & editing, Funding acquisition, Conceptualization.

Declaration of competing interest

The authors have declared no conflict of interest.

Acknowledgement

This study was supported by National Natural Science Foundation of China (82374347), Shanghai Human Resources and Social Security Bureau (Pujiang Fellowship, 2023PJD094), Health Commission of Shanghai (2022QN005, GWIV-28) and Shanghai Commission of Science and Technology (22ZR1462200).

Supplementary materials

Supplementary material associated with this article can be found, in the online version, at doi:10.1016/j.phymed.2025.157244.

References

Abbas, Z., Rehman, S., 2018. An overview of cancer treatment modalities. Neoplasm 1, 139–157.
Aghagolzadeh, P., Radpour, R., Bachtler, M., van Goor, H., Smith, E.R., Lister, A., Odermatt, A., Feelisch, M., Pasch, A., 2017. Hydrogen sulfide attenuates calcification of vascular smooth muscle cells via KEAP1/NRF2/NQO1 activation. Atherosclerosis 265, 78–86.
Alam, M.F., Khan, G., Safhi, M.M., Alshahrani, S., Siddiqui, R., Sivagurunathan Moni, S., Anwer, T., 2018. Thymoquinone ameliorates doxorubicin-induced cardiotoxicity in swiss albino mice by modulating oxidative damage and cellular inflammation. Cardiol. Res. Pr. 2018 (1), 1483041.
Aswar, U., Mahajan, U., Kandhare, A., Aswar, M., 2019. Ferulic acid ameliorates doxorubicin-induced cardiac toxicity in rats. NAUNYN-SCHMIEDEBERGS ARCHIVES OF. PHARMACOLOGY 392 (6), 659–668.
Bahar, E., Kim, H., Yoon, H., 2016. ER stress-mediated signaling: action potential and Ca (2+) as key players. Int. J. Mol. Sci 17 (9).
Bartlett, J.J., Trivedi, P.C., Pulinilkunnil, T., 2017. Autophagic dysregulation in doxorubicin cardiomyopathy. J. Mol. Cell. Cardiol 104, 1–8.
Bartlett, J.J., Trivedi, P.C., Yeung, P., Kienesberger, P.C., Pulinilkunnil, T., 2016. Doxorubicin impairs cardiomyocyte viability by suppressing transcription factor EB expression and disrupting autophagy. Biochem. J. 473 (21), 3769–3789.
Bellezza, I., Giambanco, I., Minelli, A., Donato, R., 2018. Nrf2-Keap1 signaling in oxidative and reductive stress. Biochim. Biophys. Acta. Mol. Cell. Res 1865 (5), 721–733.
Brady, O.A., Martina, J.A., Puertollano, R., 2018. Emerging roles for TFEB in the immune response and inflammation. Autophagy 14 (2), 181–189.
Bray, F., Laversanne, M., Sung, H.Y.A., Ferlay, J., Siegel, R.L., Soerjomataram, I., Jemal, A., 2024. Global cancer statistics 2022: GLOBOCAN estimates of incidence and mortality worldwide for 36 cancers in 185 countries. CA-CANCER. J. FOR. CLIN. 74 (3), 229–263.
Cargnello, M., Roux, P.P., 2011. Activation and function of the MAPKs and their substrates, the MAPK-activated protein kinases. Microbiol. Mol. Biol. Rev 75 (1), 50–83.
Carvalho, C., Santos, R.X., Cardoso, S., Correia, S., Oliveira, P.J., Santos, M.S., Moreira, P.I., 2009. Doxorubicin: the good, the bad and the ugly effect. Curr. Med. Chem 16 (25), 3267–3285.
Chabner, B.A., Roberts, T.G., 2005. Chemotherapy and the war on cancer. Nat. Rev. Cancer 5 (1), 65–72.
Chang, C., Young, L.N., Morris, K.L., von Bülow, S., Schöneberg, J., Yamamoto-Imoto, H., Oe, Y., Yamamoto, K., Nakamura, S., Stjepanovic, G., Hummer, G., Yoshimori, T.,

Hurley, J.H., 2019. Bidirectional control of autophagy by BECN1 BARA domain dynamics. Mol. Cell 73 (2), 339–353.e336.
Chen, L., Yang, T., Lu, D.W., Zhao, H., Feng, Y.L., Chen, H., Chen, D.Q., Vaziri, N.D., Zhao, Y.Y., 2018. Central role of dysregulation of TGF-β/Smad in CKD progression and potential targets of its treatment. Biomed. Pharmacother 101, 670–681.
Chen, M.P., Yang, S.H., Chou, C.H., Yang, K.C., Wu, C.C., Cheng, Y.H., Lin, F.H., 2010. The chondroprotective effects of ferulic acid on hydrogen peroxide-stimulated chondrocytes: inhibition of hydrogen peroxide-induced pro-inflammatory cytokines and metalloproteinase gene expression at the mRNA level. Inflamm. Res 59 (8), 587–595.
Chen, R.-c., Sun, G.-b., Ye, J.-x., Wang, J., Zhang, M.-d., Sun, X.-b., 2017. Salvianolic acid B attenuates doxorubicin-induced ER stress by inhibiting TRPC3 and TRPC6 mediated Ca2+ overload in rat cardiomyocytes. Toxicol. Lett 276, 21–30.
Chen, R., Sun, G., Yang, L., Wang, J., Sun, X., 2016. Salvianolic acid B protects against doxorubicin induced cardiac dysfunction via inhibition of ER stress mediated cardiomyocyte apoptosis. Toxicol. Res. (Camb) 5 (5), 1335–1345.
Chen, S., Jiang, C., Yi, X., Shu, Q., Feng, Y., Zhong, L., Huang, M., Zhu, J., Fang, L., 2025. Validated target-based network pharmacology reveals that salvianolic acid C attenuates doxorubicin-induced cardiotoxicity by regulating apoptosis and oxidative stress. Biochem. Biophys. Res. Commun 775 (.
Chen, X., Guo, J., Bao, J., Lu, J., Wang, Y., 2014. The anticancer properties of Salvia miltiorrhiza Bunge (Danshen): a systematic review. Med. Res. Rev 34 (4), 768–794.
Cheng, D., Sheng, S., Hu, J., Cai, S., Liu, Y., Gan, R., Zhu, Z., Ge, L., Chen, W., Cheng, X., 2025. Ershen Zhenwu decoction suppresses myocardial fibrosis of chronic heart failure with heart-kidney yang deficiency by down-regulating the Ras Homolog Gene Family Member A/Rho-Associated Coiled-Coil kinases signaling pathway. J. Ethnopharmacol 340, 119146.
Childs, A.C., Phaneuf, S.L., Dirks, A.J., Phillips, T., Leeuwenburgh, C., 2002. Doxorubicin treatment in vivo causes cytochrome C release and cardiomyocyte apoptosis, as well as increased mitochondrial efficiency, superoxide dismutase activity, and bcl-2:bax ratio. Cancer. Res 62 (16), 4592–4598.
Chiu, T.L., Su, C.C., 2010. Tanshinone IIA induces apoptosis in human lung cancer A549 cells through the induction of reactive oxygen species and decreasing the mitochondrial membrane potential. Int. J. Mol. Med 25 (2), 231–236.
Chotenimitkhun, R., D'Agostino Jr., R., Lawrence, J.A., Hamilton, C.A., Jordan, J.H., Vasu, S., Lash, T.L., Yeboah, J., Herrington, D.M., Hundley, W.G., 2015. Chronic statin administration may attenuate early anthracycline-associated declines in left ventricular ejection function. Can. J. Cardiol 31 (3), 302–307.
Chowanadisai, W., Bauerly, K.A., Tchaparian, E., Wong, A., Cortopassi, G.A., Rucker, R. B., 2010. Pyrroloquinoline quinone stimulates mitochondrial biogenesis through cAMP response element-binding protein phosphorylation and increased PGC-1alpha expression. J. Biol. Chem 285 (1), 142–152.
Committee, C.P., 2020. The Chinese Pharmacopoeia 2020 edition, Traditional Chinese medicines including materials, cut crude drugs, vegetable olils and extracts, formulation preparation and single flavour preparaton. China Medical Science and Technology Press, Beijing, China.
Cove-Smith, L., Woodhouse, N., Hargreaves, A., Kirk, J., Smith, S., Price, S.A., Galvin, M., Betts, C.J., Brocklehurst, S., Backen, A., Radford, J., Linton, K., Roberts, R.A., Schmitt, M., Dive, C., Tugwood, J.D., Hockings, P.D., Mellor, H.R., 2014. An integrated characterization of serological, pathological, and functional events in doxorubicin-induced cardiotoxicity. Toxicol. Sci. 140 (1), 3–15.
Davies, K.J., Doroshow, J.H., 1986. Redox cycling of anthracyclines by cardiac mitochondria. I. Anthracycline radical formation by NADH dehydrogenase. J. Biol. Chem 261 (7), 3060–3067.
Deng, L., Huang, L., Guo, Q., Shi, X., Xu, K., 2017. CREB1 and Smad3 mediate TGF-β3-induced Smad7 expression in rat hepatic stellate cells. Mol. Med. Rep 16 (6), 8455–8462.
Di Nardo, P., Lisanti, C., Garutti, M., Buriolla, S., Alberti, M., Mazzeo, R., Puglisi, F., 2022. Chemotherapy in patients with early breast cancer: clinical overview and management of long-term side effects. Expert. Opin. Drug. Saf 21 (11), 1341–1355.
Dill, T.L., Naya, F.J., 2018. A hearty dose of noncoding RNAs: the imprinted DLK1-DIO3 locus in cardiac development and disease. J. Cardiovasc. Dev. Dis 5 (3).
Dong, M., Hu, N., Hua, Y., Xu, X., Kandadi, M.R., Guo, R., Jiang, S., Nair, S., Hu, D., Ren, J., 2013. Chronic Akt activation attenuated lipopolysaccharide-induced cardiac dysfunction via Akt/GSK3β-dependent inhibition of apoptosis and ER stress. Biochim. Biophys. Acta. (BBA). -. Mol. Basis. Dis. 1832 (6), 848–863.
Du, Q., Zhu, B., Zhai, Q., Yu, B., 2017. Sirt3 attenuates doxorubicin-induced cardiac hypertrophy and mitochondrial dysfunction via suppression of Bnip3. Am. J. Transl. Res 9 (7), 3360–3373.
Fa, H.G., Chang, W.G., Zhang, X.J., Xiao, D.D., Wang, J.X., 2021. Noncoding RNAs in doxorubicin-induced cardiotoxicity and their potential as biomarkers and therapeutic targets. Acta. Pharmacol. Sin 42 (4), 499–507.
Feng, K., Liu, Y., Sun, J., Zhao, C., Duan, Y., Wang, W., Yan, K., Yan, X., Sun, H., Hu, Y., Han, J., 2021. Compound Danshen dripping pill inhibits doxorubicin or isoproterenol-induced cardiotoxicity. BIOMED. PHARMACOTHER. 138.
Feng, X., Li, Y., Wang, Y., Li, L., Little, P.J., Xu, S.W., Liu, S., 2019. Danhong injection in cardiovascular and cerebrovascular diseases: pharmacological actions, molecular mechanisms, and therapeutic potential. Pharmacol. Res 139, 62–75.
Feng, Y., Niu, L.L., Wei, W., Zhang, W.Y., Li, X.Y., Cao, J.H., Zhao, S.H., 2013. A feedback circuit between miR-133 and the ERK1/2 pathway involving an exquisite mechanism for regulating myoblast proliferation and differentiation. Cell. Death. Dis 4 (11), e934.
Filho, A.M., Laversanne, M., Ferlay, J., Colombet, M., Piñeros, M., Znaor, A., Parkin, D. M., Soerjomataram, I., Bray, F., 2025. The GLOBOCAN 2022 cancer estimates: data sources, methods, and a snapshot of the cancer burden worldwide. Int. J. Cancer 156 (7), 1336–1346.
Gao, H., Liu, X., Sun, W., Kang, N., Liu, Y., Yang, S., Xu, Q.M., Wang, C., Chen, X., 2017. Total tanshinones exhibits anti-inflammatory effects through blocking TLR4 dimerization via the MyD88 pathway. Cell. Death. Dis 8 (8), e3004.
Gao, H., Sun, W., Zhao, J., Wu, X., Lu, J.J., Chen, X., Xu, Q.M., Khan, I.A., Yang, S., 2016. Tanshinones and diethyl blechnics with anti-inflammatory and anti-cancer activities from Salvia miltiorrhiza Bunge (Danshen). Sci. Rep 6, 33720.
Gao, J., Yang, G., Pi, R., Li, R., Wang, P., Zhang, H., Le, K., Chen, S., Liu, P., 2008. Tanshinone IIA protects neonatal rat cardiomyocytes from adriamycin-induced apoptosis. TRANSL. RES. 151 (2), 79–87.
Ge, W., Zhang, X., Lin, J., Wang, Y., Zhang, X., Duan, Y., Dai, X., Zhang, J., Zhang, Y., Jiang, M., Qiang, H., Zhao, Z., Zhang, X., Sun, D., 2025. Rnd3 protects against doxorubicin-induced cardiotoxicity through inhibition of PANoptosis in a Rock1/Drp1/mitochondrial fission-dependent manner. Cell. Death. Dis 16 (1), 2.
Ghanem, A., Emara, H.A, Muawia, S., Abd El Maksoud, A.I., Al-Karmalawy, A.A., Elshal, M.F., 2020. Tanshinone IIA synergistically enhances the antitumor activity of doxorubicin by interfering with the PI3K/AKT/mTOR pathway and inhibition of topoisomerase II:in vitroand molecular docking studies. New. J. Chem. 44 (40), 17374–17381.
Griffin-Green, E.A., Zaleska, M.M., Erecińska, M., 1988. Adriamycin-induced lipid peroxidation in mitochondria and microsomes. Biochem. Pharmacol 37 (16), 3071–3077.
Guo, J., Yong, Y., Aa, J., Cao, B., Sun, R., Yu, X., Huang, J., Yang, N., Yan, L., Li, X., Cao, J., Aa, N., Yang, Z., Kong, X., Wang, L., Zhu, X., Ma, X., Guo, Z., Zhou, S., Sun, H., Wang, G., 2016. Compound danshen dripping pills modulate the perturbed energy metabolism in a rat model of acute myocardial ischemia. Sci. Rep 6, 37919.
Guo, Z., Yan, M., Chen, L., Fang, P., Li, Z., Wan, Z., Cao, S., Hou, Z., Wei, S., Li, W., Zhang, B., 2018. Nrf2-dependent antioxidant response mediated the protective effect of tanshinone IIA on doxorubicin-induced cardiotoxicity. Exp. Ther. Med 16 (4), 3333–3344.
Gurkar, A.U., Chu, K., Raj, L., Bouley, R., Lee, S.-H., Kim, Y.-B., Dunn, S.E., Mandinova, A., Lee, S.W., 2013. Identification of ROCK1 kinase as a critical regulator of Beclin1-mediated autophagy during metabolic stress. Nat. Commun 4 (1), 2189.
Han, J.Y., Fan, J.Y., Horie, Y., Miura, S., Cui, D.H., Ishii, H., Hibi, T., Tsuneki, H., Kimura, I., 2008. Ameliorating effects of compounds derived from Salvia miltiorrhiza root extract on microcirculatory disturbance and target organ injury by ischemia and reperfusion. Pharmacol. Ther 117 (2), 280–295.
Hao, Y., Xie, T., Korotcov, A., Zhou, Y., Pang, X., Shan, L., Ji, H., Sridhar, R., Wang, P., Califano, J., Gu, X., 2009. Salvianolic acid B inhibits growth of head and neck squamous cell carcinoma in vitro and in vivo via cyclooxygenase-2 and apoptotic pathways. Int. J. Cancer 124 (9), 2200–2209.
Hardie, D.G., 2003. Minireview: the AMP-activated protein kinase cascade: the key sensor of cellular energy status. Endocrinology 144 (12), 5179–5183.
Hong, H.-J., Liu, J.-C., Chen, P.-Y., Chen, J.-J., Chan, P., Cheng, T.-H., 2012. Tanshinone IIA prevents doxorubicin-induced cardiomyocyte apoptosis through Akt-dependent pathway. Int. J. Cardiol 157 (2), 174–179.
Hong, L.L., Zhao, Y., Chen, W.D., Yang, C.Y., Li, G.Z., Wang, H.S., Cheng, X.Y., 2022. Tentative exploration of pharmacodynamic substances: pharmacological effects, chemical compositions, and multi-components pharmacokinetic characteristics of ESZWD in CHF-HKYd rats. Front. Cardiovasc. Med 9, 913661.
Hooijmans, C.R., Rovers, M.M., de Vries, R.B., Leenaars, M., Ritskes-Hoitinga, M., Langendam, M.W., 2014. SYRCLE's risk of bias tool for animal studies. BMC. Med. Res. Methodol 14, 43.
Huang, K.M., Zavorka Thomas, M., Magdy, T., Eisenmann, E.D., Uddin, M.E., DiGiacomo, D.F., Pan, A., Keiser, M., Otter, M., Xia, S.H., Li, Y., Jin, Y., Fu, Q., Gibson, A.A., Bonilla, I.M., Carnes, C.A., Corps, K.N., Coppola, V., Smith, S.A., Addison, D., Nies, A.T., Bundschuh, R., Chen, T., Lustberg, M.B., Wang, J., Oswald, S., Campbell, M.J., Yan, P.S., Baker, S.D., Hu, S., Burridge, P.W., Sparreboom, A., 2021a. Targeting OCT3 attenuates doxorubicin-induced cardiac injury. Proc. Natl. Acad. Sci. U. S. A 118 (5).
Huang, R., Zhou, P.K., 2021. DNA damage repair: historical perspectives, mechanistic pathways and clinical translation for targeted cancer therapy. Signal. Transduct. Target. Ther 6 (1), 254.
Huang, Y., Yu, S.H., Zhen, W.X., Cheng, T., Wang, D., Lin, J.B., Wu, Y.H., Wang, Y.F., Chen, Y., Shu, L.P., Wang, Y., Sun, X.J., Zhou, Y., Yang, F., Hsu, C.H., Xu, P.F., 2021b. Tanshinone I, a new EZH2 inhibitor restricts normal and malignant hematopoiesis through upregulation of MMP9 and ABCG2. Theranostics 11 (14), 6891–6904.
Hung, Y.C., Wang, P.W., Lin, T.Y., Yang, P.M., You, J.S., Pan, T.L., 2020. Functional redox proteomics reveal that salvia miltiorrhiza aqueous extract alleviates adriamycin-induced cardiomyopathy via inhibiting ROS-dependent apoptosis. Oxid. Med. Cell. Longev 2020, 5136934.
Imam, F., Al-Harbi, N.O., Al-Harbi, M.M., Ansari, M.A., Al-Asmari, A.F., Ansari, M.N., Al-Anazi, W.A., Bahashwan, S., Almutairi, M.M., Alshammari, M., Khan, M.R., Alsaad, A.M., Alotaibi, M.R., 2018. Apremilast prevent doxorubicin-induced apoptosis and inflammation in heart through inhibition of oxidative stress mediated activation of NF-κb signaling pathways. Pharmacol. Rep 70 (5), 993–1000.
Jacobs, K.M., Bhave, S.R., Ferraro, D.J., Jaboin, J.J., Hallahan, D.E., Thotala, D., 2012. GSK-3β: A bifunctional role in cell death pathways. Int. J. Cell. Biol 2012 (1), 930710.
Ji, X.Y., Tan, B.K., Zhu, Y.Z., 2000. Salvia miltiorrhiza and ischemic diseases. Acta. Pharmacol. Sin 21 (12), 1089–1094.
Jiang, B., Zhang, L., Li, M., Wu, W., Yang, M., Wang, J., Guo, D.-a, 2008. Salvianolic acids prevent acute doxorubicin cardiotoxicity in mice through suppression of oxidative stress. FOOD. AND. CHEM. TOXICOL. 46 (5), 1510–1515.

Jiang, B., Zhang, L., Wang, Y., Li, M., Wu, W., Guan, S., Liu, X., Yang, M., Wang, J., Guo, D.-a., 2009. Tanshinone IIA sodium sulfonate protects against cardiotoxicity induced by doxorubicin in vitro and in vivo. FOOD. AND. CHEM. TOXICOL. 47 (7), 1538–1544.
Jiang, Q.-q., Zhang, J.-m., Xue, S.-m., Tian, X., Chen, X., Liu, T.-t., Jiang, Y.-y., Sun, Q.-b., Guo, D.-q., Li, C., Wang, Y., Wang, Q.-y., 2022a. Tanshinone I attenuates doxorubicin-induced cardiotoxicity based on the akt-Nrf2 antioxidant pathway. Yaoxue. Xuebao 57 (10), 3077–3085.
Jiang, Q., Chen, X., Tian, X., Zhang, J., Xue, S., Jiang, Y., Liu, T., Wang, X., Sun, Q., Hong, Y., Li, C., Guo, D., Wang, Y., Wang, Q., 2022b. Tanshinone I inhibits doxorubicin-induced cardiotoxicity by regulating Nrf2 signaling pathway. PHYTOMEDICINE 106.
Kadenbach, B., Ramzan, R., Moosdorf, R., Vogt, S., 2011. The role of mitochondrial membrane potential in ischemic heart failure. Mitochondrion 11 (5), 700–706.
Kania, G., Blyszczuk, P., Eriksson, U., 2009. Mechanisms of cardiac fibrosis in inflammatory heart disease. Trends. Cardiovasc. Med 19 (8), 247–252.
Kciuk, M., Gielecińska, A., Mujwar, S., Kołat, D., Kałuzińska-Kołat, Ż., Celik, I., Kontek, R., 2023. Doxorubicin-an agent with multiple mechanisms of anticancer activity. Cells 12 (4).
Lee, C.Y., Sher, H.F., Chen, H.W., Liu, C.C., Chen, C.H., Lin, C.S., Yang, P.C., Tsay, H.S., Chen, J.J., 2008. Anticancer effects of tanshinone I in human non-small cell lung cancer. Mol. Cancer. Ther 7 (11), 3527–3538.
Lennicke, C., Rahn, J., Heimer, N., Lichtenfels, R., Wessjohann, L.A., Seliger, B., 2016. Redox proteomics: methods for the identification and enrichment of redox-modified proteins and their applications. Proteomics 16 (2), 197–213.
Li, C., Wang, J., Wang, Q., Zhang, Y., Zhang, N., Lu, L., Wu, Y., Zhang, Q., Wang, W., Wang, Y., Tu, P., 2016a. Qishen granules inhibit myocardial inflammation injury through regulating arachidonic acid metabolism. Sci. Rep 6 (1), 36949.
Li, D.L., Wang, Z.V., Ding, G., Tan, W., Luo, X., Criollo, A., Xie, M., Jiang, N., May, H., Kyrychenko, V., Schneider, J.W., Gillette, T.G., Hill, J.A., 2016b. Doxorubicin blocks cardiomyocyte autophagic flux by inhibiting lysosome acidification. Circulation 133 (17), 1668–1687.
Li, G.-H., Li, Y.-R., Jiao, P., Zhao, Y., Hu, H.-X., Lou, H.-X., Shen, T., 2018a. Therapeutic potential of Salviae miltiorrhizae radix et rhizoma against Human diseases based on activation of Nrf2-mediated antioxidant defense system: bioactive constituents and mechanism of action. Oxid. Med. Cell. Longev 2018, 7309073.
Li, J., Zhang, Y., Zuo, Z., Zhang, Z., Wang, Y., Chang, S., Huang, J., Dai, Y., Ge, J., 2024a. Salvianolate injection ameliorates cardiomyopathy by regulating autophagic flux through miR-30a/becn1 axis in zebrafish. Chin. Med. J. (Engl).
Li, L., Wu, B., Zhao, Q., Lie, J., Han, Y., Fan, X., Dong, J., Li, P., 2020. Attenuation of doxorubicin-induced cardiotoxicity by cryptotanshinone detected through association analysis of transcriptomic profiling and KEGG pathway. Aging-Us 12 (10), 9585–9603.
Li, Y., Gao, G., Han, Y., Xiao, B., Shen, L., Yang, X., Liu, Y., Mu, Y., Zhang, N., Niu, C., Wang, Y., 2024b. Rho kinase inhibitor Y-27632 downregulates IL-1β expression in mice with experimental autoimmune myocarditis. Sci. Rep 14 (1), 9763.
Li, Z.M., Xu, S.W., Liu, P.Q., 2018b. Salvia miltiorrhizaBurge (Danshen): a golden herbal medicine in cardiovascular therapeutics. Acta. Pharmacol. Sin 39 (5), 802–824.
Lien, C.Y., Chuang, T.Y., Hsu, C.H., Lin, C.L., Wang, S.E., Sheu, S.J., Chien, C.T., Wu, C. H., 2015. Oral treatment with the herbal formula B307 alleviates cardiac toxicity in doxorubicin-treated mice via suppressing oxidative stress, inflammation, and apoptosis. Onco. Targets. Ther 8, 1193–1210.
Liu, J., Fu, M., Wang, M., Wan, D., Wei, Y., Wei, X., 2022. Cancer vaccines as promising immuno-therapeutics: platforms and current progress. J. Hematol. Oncol 15 (1), 28.
Liu, Y., Zhang, D.T., Liu, X.G., 2015. mTOR signaling in T cell immunity and autoimmunity. Int. Rev. Immunol 34 (1), 50–66.
Lopez de Vergara, O., Pablos, R., Ruiz-Sanz, M.B., Ruiz-Larrea, J.I., Navarro, R., 2014. Characterization of the NF-?B signaling triggered by doxorubicin. Free. Radic. Biol. Med 75 (Suppl 1), S38.
Lu, W., Wang, Y., Wen, J., 2024. The roles of RhoA/ROCK/NF-κb pathway in microglia polarization following ischemic stroke. J. Neuroimmune. Pharmacol. 19 (1), 19.
Luo, J., Song, W., Yang, G., Xu, H., Chen, K., 2015. Compound Danshen (Salvia miltiorrhiza) dripping pill for coronary heart disease: an overview of systematic reviews. Am. J. Chin. Med 43 (1), 25–43.
Ma, L., Tang, L., Yi, Q., 2019. Salvianolic acids: potential source of natural drugs for the treatment of fibrosis disease and cancer. Front. Pharmacol 10, 97.
Ma, Y., Mouton, A.J., Lindsey, M.L., 2018. Cardiac macrophage biology in the steady-state heart, the aging heart, and following myocardial infarction. Transl. Res 191, 15–28.
Mao, W., Iwai, C., Liu, J., Sheu, S.-S., Fu, M., Liang, C.-s., 2008. Darbepoetin alfa exerts a cardioprotective effect in autoimmune cardiomyopathy via reduction of ER stress and activation of the PI3K/Akt and STAT3 pathways. J. Mol. Cell. Cardiol 45 (2), 250–260.
Mihaylova, M.M., Shaw, R.J., 2011. The AMPK signalling pathway coordinates cell growth, autophagy and metabolism. Nat. Cell. Biol 13 (9), 1016–1023.
Mitry, M.A., Edwards, J.G., 2016. Doxorubicin induced heart failure: phenotype and molecular mechanisms. Int. J. Cardiol. Heart. Vasc 10, 17–24.
Nishiyama, K., Tanaka, T., Nishimura, A., Nishida, M., 2021. TRPC3-Based protein signaling complex as a therapeutic target of myocardial atrophy. Curr. Mol. Pharmacol 14 (2), 123–131.
Nizamutdinova, I.T., Lee, G.W., Son, K.H., Jeon, S.J., Kang, S.S., Kim, Y.S., Lee, J.H., Seo, H.G., Chang, K.C., Kim, H.J., 2008. Tanshinone I effectively induces apoptosis in estrogen receptor-positive (MCF-7) and estrogen receptor-negative (MDA-MB-231) breast cancer cells. Int. J. Oncol 33 (3), 485–491.
Nohl, H., Jordan, W., 1983. OH•-generation by adriamycin semiquinone and H2O2; an explanation for the cardiotoxicity of anthracycline antibiotics. Biochem. Biophys. Res. Commun 114 (1), 197–205.
Octavia, Y., Tocchetti, C.G., Gabrielson, K.L., Janssens, S., Crijns, H.J., Moens, A.L., 2012. Doxorubicin-induced cardiomyopathy: from molecular mechanisms to therapeutic strategies. J. Mol. Cell. Cardiol 52 (6), 1213–1225.
Ogura, R., Sugiyama, M., Haramaki, N., Hidaka, T., 1991. Electron spin resonance studies on the mechanism of adriamycin-induced heart mitochondrial damages. Cancer. Res 51 (13), 3555–3558.
Oh, K.S., Oh, B.K., Mun, J., Seo, H.W., Lee, B.H., 2011. Salvianolic acid A suppress lipopolysaccharide-induced NF-κb signaling pathway by targeting ikkβ. Int. Immunopharmacol 11 (11), 1901–1906.
Orogo, A.M., Gustafsson, Å.B., 2015. Therapeutic targeting of autophagy. Circ. Res 116 (3), 489–503.
Pabla, N., Dong, Z., 2012. Curtailing side effects in chemotherapy: a tale of pkcδ in cisplatin treatment. Oncotarget 3 (1), 107–111.
Page, M.J., McKenzie, J.E., Bossuyt, P.M., Boutron, I., Hoffmann, T.C., Mulrow, C.D., Shamseer, L., Tetzlaff, J.M., Akl, E.A., Brennan, S.E., Chou, R., Glanville, J., Grimshaw, J.M., Hróbjartsson, A., Lalu, M.M., Li, T., Loder, E.W., Mayo-Wilson, E., McDonald, S., McGuinness, L.A., Stewart, L.A., Thomas, J., Tricco, A.C., Welch, V.A., Whiting, P., Moher, D., 2021. The PRISMA 2020 statement: an updated guideline for reporting systematic reviews. Rev. Esp. Cardiol. (Engl. Ed) 74 (9), 790–799.
Pérez-Herrero, E., Fernández-Medarde, A., 2015. Advanced targeted therapies in cancer: drug nanocarriers, the future of chemotherapy. Eur. J. Pharm. Biopharm 93, 52–79.
Pugazhendhi, A., Edison, T., Velmurugan, B.K., Jacob, J.A., Karuppusamy, I., 2018. Toxicity of doxorubicin (Dox) to different experimental organ systems. Life. Sci 200, 26–30.
Qi, J.-y., Yang, Y.-k., Jiang, C., Zhao, Y., Wu, Y.-c., Han, X., Jing, X., Wu, Z.-l., Chu, L., 2022. Exploring the mechanism of Danshensu in the treatment of doxorubicin-induced cardiotoxicity based on network pharmacology and experimental evaluation. FRONT. IN. CARDIOVASC. MED. 9.
Rajagopalan, S., Politi, P.M., Sinha, B.K., Myers, C.E., 1988. Adriamycin-induced free radical formation in the perfused rat heart: implications for cardiotoxicity. Cancer. Res 48 (17), 4766–4769.
Ramalingam, L., Menikdiwela, K., LeMieux, M., Dufour, J.M., Kaur, G., Kalupahana, N., Moustaid-Moussa, N., 2017. The renin angiotensin system, oxidative stress and mitochondrial function in obesity and insulin resistance. Biochim. Biophys. Acta - Mol. Basis Dis. 1863 (5), 1106–1114.
Rao, S., Mondragón, L., Pranjic, B., Hanada, T., Stoll, G., Köcher, T., Zhang, P., Jais, A., Lercher, A., Bergthaler, A., Schramek, D., Haigh, K., Sica, V., Leduc, M., Modjtahedi, N., Pai, T.-P., Onji, M., Uribesalgo, I., Hanada, R., Kozieradzki, I., Koglgruber, R., Cronin, S.J., She, Z., Quehenberger, F., Popper, H., Kenner, L., Haigh, J.J., Kepp, O., Rak, M., Cai, K., Kroemer, G., Penninger, J.M., 2019. AIF-regulated oxidative phosphorylation supports lung cancer development. Cell. Res 29 (7), 579–591.
Ren, J., Fu, L., Nile, S.H., Zhang, J., Kai, G., 2019. Salvia miltiorrhiza in treating cardiovascular diseases: A review on its pharmacological and clinical applications. Front. Pharmacol 10, 753.
Renu, K., V, G.A., P, B.T., Arunachalam, S., 2018. Molecular mechanism of doxorubicin-induced cardiomyopathy - an update. Eur. J. Pharmacol 818, 241–253.
Roca-Alonso, L., Castellano, L., Mills, A., Dabrowska, A.F., Sikkel, M.B., Pellegrino, L., Jacob, J., Frampton, A.E., Krell, J., Coombes, R.C., Harding, S.E., Lyon, A.R., Stebbing, J., 2015. Myocardial MiR-30 downregulation triggered by doxorubicin drives alterations in β-adrenergic signaling and enhances apoptosis. Cell. Death. Dis 6 (5) e1754-e1754.
Ron, D., Walter, P., 2007. Signal integration in the endoplasmic reticulum unfolded protein response. Nat. Rev. Mol. Cell. Biol 8 (7), 519–529.
Ross, D., Siegel, D., 2021. The diverse functionality of NQO1 and its roles in redox control. Redox. Biol 41, 101950.
Sahan-Firat, S., Temiz-Resitoglu, M., Guden, D.S., Kucukkavruk, S.P., Tunctan, B., Sari, A.N., Kocak, Z., Malik, K.U., 2018. Protection by mTOR inhibition on zymosan-induced systemic inflammatory response and oxidative/nitrosative stress: contribution of mTOR/MEK1/ERK1/2/ikkβ/iκb-α/NF-κb signalling pathway. Inflammation 41 (1), 276–298.
Scarpulla, R.C., 2002. Nuclear activators and coactivators in mammalian mitochondrial biogenesis. Biochim. Biophys. Acta 1576 (1-2), 1–14.
Senft, D., Ronai, Z.A., 2015. UPR, autophagy, and mitochondria crosstalk underlies the ER stress response. Trends. Biochem. Sci 40 (3), 141–148.
Shimizu, T., Liao, J.K., 2016. Rho Kinases and cardiac remodeling. Circ. J. 80 (7), 1491–1498.
Siegel, R.L., Kratzer, T.B., Giaquinto, A.N., Sung, H., Jemal, A., 2025. Cancer statistics, 2025. CA. Cancer. J. Clin 75 (1), 10–45.
Sishi, B.J., Loos, B., van Rooyen, J., Engelbrecht, A.M., 2013. Doxorubicin induces protein ubiquitination and inhibits proteasome activity during cardiotoxicity. Toxicology 309, 23–29.
Song, T., Yao, Y., Wang, T., Huang, H., Xia, H., 2017. Tanshinone IIA ameliorates apoptosis of myocardiocytes by up-regulation of miR-133 and suppression of caspase-9. Eur. J. Pharmacol 815, 343–350.
Songbo, M., Lang, H., Xinyong, C., Bin, X., Ping, Z., Liang, S., 2019. Oxidative stress injury in doxorubicin-induced cardiotoxicity. Toxicol. Lett 307, 41–48.
Stěrba, M., Popelová, O., Vávrová, A., Jirkovský, E., Kovaříková, P., Geršl, V., Simůnek, T., 2013. Oxidative stress, redox signaling, and metal chelation in anthracycline cardiotoxicity and pharmacological cardioprotection. Antioxid. Redox. Signal 18 (8), 899–929.
Su, C.Y., Ming, Q.L., Rahman, K., Han, T., Qin, L.P., 2015. Salvia miltiorrhiza: traditional medicinal uses, chemistry, and pharmacology. Chin. J. Nat. Med 13 (3), 163–182.

Sun, F., Zhou, Q., Pang, X., Xu, Y., Rao, Z., 2013. Revealing various coupling of electron transfer and proton pumping in mitochondrial respiratory chain. Curr. Opin. Struct. Biol 23 (4), 526–538.
Sun, W., Liu, Q., Leng, J., Zheng, Y., Li, J., 2015. The role of Pyruvate dehydrogenase Complex in cardiovascular diseases. Life. Sci 121, 97–103.
Sun, X., Chen, G., Xie, Y., Jiang, D., Han, J., Chen, F., Song, Y., 2020. Qiliqiangxin improves cardiac function and attenuates cardiac remodelling in doxorubicin-induced heart failure rats. Pharm. Biol 58 (1), 417–426.
Tadokoro, T., Ikeda, M., Ide, T., Deguchi, H., Ikeda, S., Okabe, K., Ishikita, A., Matsushima, S., Koumura, T., Yamada, K.I., Imai, H., Tsutsui, H., 2020. Mitochondria-dependent ferroptosis plays a pivotal role in doxorubicin cardiotoxicity. JCI. Insight 5 (9).
Taefehshokr, N., Baradaran, B., Baghbanzadeh, A., Taefehshokr, S., 2020. Promising approaches in cancer immunotherapy. Immunobiology 225 (2), 151875.
Tai, Y., Yang, S., Liu, Y., Shao, W., 2017. TRPC channels in health and disease. Adv. Exp. Med. Biol 976, 35–45.
Tang, W.H.W., Huang, Y., 2013. Cardiotonic modulation in heart failure: insights from traditional Chinese medicine. J. Am. Coll. Cardiol 62 (12), 1073–1074.
Thapa, N., Chen, M., Horn, H.T., Choi, S., Wen, T., Anderson, R.A., 2020. Phosphatidylinositol 3-kinase signalling is spatially organized at endosomal compartments by microtubule-associated protein 4. Nat. Cell Biol. 22 (11), 1357–1370.
Timm, K.N., Tyler, D.J., 2020. The role of AMPK activation for cardioprotection in doxorubicin-induced cardiotoxicity. Cardiovasc. Drugs. Ther. 34 (2), 255–269.
Vallejo, M.J., Salazar, L., Grijalva, M., 2017. Oxidative stress modulation and ROS-mediated toxicity in cancer: A review on In vitro models for plant-derived compounds. Oxid. Med. Cell. Longev 2017, 4586068.
Vara, J.Á.F., Casado, E., de Castro, J., Cejas, P., Belda-Iniesta, C., González-Barón, M., 2004. PI3K/akt signalling pathway and cancer. Cancer. Treat. Rev 30 (2), 193–204.
Viskupicova, J., Rezbarikova, P., 2022. Natural polyphenols as SERCA activators: role in the endoplasmic reticulum stress-related diseases. Molecules 27 (16), 5095.
Wang, X., Li, C., Wang, Q., Li, W., Guo, D., Zhang, X., Shao, M., Chen, X., Ma, L., Zhang, Q., Wang, W., Wang, Y., 2019a. Tanshinone IIA restores dynamic balance of autophagosome/autolysosome in doxorubicin-induced cardiotoxicity via targeting Beclin1/LAMP1. Cancers. (Basel) 11 (7).
Wang, X., Morris-Natschke, S.L., Lee, K.H., 2007. New developments in the chemistry and biology of the bioactive constituents of Tanshen. Med. Res. Rev 27 (1), 133–148.
Wang, X., Sun, Q., Jiang, Q., Jiang, Y., Zhang, Y., Cao, J., Lu, L., Li, C., Wei, P., Wang, Q., Wang, Y., 2021a. Cryptotanshinone ameliorates doxorubicin-induced cardiotoxicity by targeting akt-GSK-3β-mPTP pathway In vitro. Molecules 26 (5).
Wang, X., Wang, Q., Li, W., Zhang, Q., Jiang, Y., Guo, D., Sun, X., Lu, W., Li, C., Wang, Y., 2020a. TFEB-NF-kappa B inflammatory signaling axis: a novel therapeutic pathway of dihydrotanshinone I in doxorubicin-induced cardiotoxicity. J. Exp. Clin. Cancer. Res. 39 (1).
Wang, X., Yang, Y., Liu, X., Gao, X., 2020b. Chapter two - pharmacological properties of tanshinones, the natural products from Salvia miltiorrhiza. In: Du, G. (Ed.), Advances in Pharmacology. Academic Press, pp. 43–70.
Wang, Y., Li, X., Wang, X., Lau, W., Wang, Y., Xing, Y., Zhang, X., Ma, X., Gao, F., 2013. Ginsenoside Rd attenuates myocardial ischemia/reperfusion injury via akt/GSK-3β signaling and inhibition of the mitochondria-dependent apoptotic pathway. PLoS. One 8 (8), e70956.
Wang, Y., Xu, F., Chen, J., Shen, X., Deng, Y., Xu, L., Yin, J., Chen, H., Teng, F., Liu, X., Wu, W., Jiang, B., Guo, D.A., 2011. Matrix metalloproteinase-9 induces cardiac fibroblast migration, collagen and cytokine secretion: inhibition by salvianolic acid B from Salvia miltiorrhiza. Phytomedicine 19 (1), 13–19.
Wang, Z., Wan, H., Tong, X., He, Y., Yang, J., Zhang, L., Shao, C., Ding, Z., Wan, H., Li, C., 2021b. An integrative strategy for discovery of functional compound combination from Traditional Chinese Medicine: Danhong Injection as a model. Biomed. Pharmacother 138, 111451.
Wang, Z., Xu, Q., Xiao, H., Yuan, L., 2019b. Tanshinone IIA attenuates doxorubicin-induced injury in H9c2 cardiomyocytes via AMPK-mediated autophagy. Chin. J. Pathophysiol. 35 (3), 406–410.
Wenningmann, N., Knapp, M., Ande, A., Vaidya, T.R., Ait-Oudhia, S., 2019. Insights into doxorubicin-induced cardiotoxicity: molecular mechanisms, preventive strategies, and early monitoring. Mol. Pharmacol 96 (2), 219–232.
Wu, Q.J., Zhang, T.N., Chen, H.H., Yu, X.F., Lv, J.L., Liu, Y.Y., Liu, Y.S., Zheng, G., Zhao, J.Q., Wei, Y.F., Guo, J.Y., Liu, F.H., Chang, Q., Zhang, Y.X., Liu, C.G., Zhao, Y. H., 2022. The sirtuin family in health and disease. Signal. Transduct. Target. Ther 7 (1), 402.
Wu, Y., Xiu, W., Wu, Y., 2021. Salvianolic Acid A protects H9C2 cardiomyocytes from doxorubicin- induced damage by inhibiting NFKB1 expression thereby downregulating long-noncoding RNA (lncRNA) plasmacytoma variant translocation 1 (PVT1). Med. Sci. Monit 27.
Wu, Z.-j., Yu, J., Wang, R.-x., Fang, Q.-j., Lin, M.-j., 2014. Protective effect of ferulic acid on doxorubicin induced cellular injury in H9c2 myocardial cells. Chin. Pharmacol. Bull. 30 (8), 1059–1065.
Xie, Z., Zhao, M., Yan, C., Kong, W., Lan, F., Narengaowa, Zhao, S., Yang, Q., Bai, Z., Qing, H., Ni, J., 2023. Cathepsin B in programmed cell death machinery: mechanisms of execution and regulatory pathways. Cell. Death. Dis 14 (4), 255.
Xu, A., Deng, F., Chen, Y., Kong, Y., Pan, L., Liao, Q., Rao, Z., Xie, L., Yao, C., Li, S., Zeng, X., Zhu, X., Liu, H., Gao, N., Xue, L., Chen, F., Xu, G., Wei, D., Zhou, X., Li, Z., Sheng, X., 2020. NF-κb pathway activation during endothelial-to-mesenchymal transition in a rat model of doxorubicin-induced cardiotoxicity. Biomed. Pharmacother. 130, 110525.
Xu, C., Xi, T., 2009. Anti-migration and anti-angiogenic effects of tanshinone IIA on breast cancer cell MDA-MB-435. J. China. Pharm. Univ. 40, 565–570.
Xu, L., Deng, Y., Feng, L., Li, D., Chen, X., Ma, C., Liu, X., Yin, J., Yang, M., Teng, F., Wu, W., Guan, S., Jiang, B., Guo, D., 2011. Cardio-protection of salvianolic acid B through inhibition of apoptosis network. PLoS. One 6 (9), e24036.
Xu, L., He, D., Wu, Y., Shen, L., Wang, Y., Xu, Y., 2022a. Tanshinone IIA inhibits cardiomyocyte apoptosis and rescues cardiac function during doxorubicin-induced cardiotoxicity by activating the DAXX/MEK/ERK1/2 pathway. PHYTOMEDICINE 107.
Xu, Z., Hu, Z., Xu, H., Zhang, L., Li, L., Wang, Y., Zhu, Y., Yang, L., Hu, D., 2022b. Liquiritigenin alleviates doxorubicin-induced chronic heart failure via promoting ARHGAP18 and suppressing RhoA/ROCK1 pathway. Exp. Cell. Res 411 (2), 113008.
Xue, S., Chen, H., Zhang, J., Tian, R., Xie, C., Sun, Q., Wang, H., Shi, T., Guo, D., Wang, Y., Wang, Q., 2024. Qishen granule alleviates doxorubicin-induced cardiotoxicity by suppressing ferroptosis via nuclear erythroid factor 2-related factor 2 (Nrf2) pathway. J. Ethnopharmacol 335, 118604.
Yang, L., Zhao, D., Ren, J., Yang, J., 2015. Endoplasmic reticulum stress and protein quality control in diabetic cardiomyopathy. Biochim. Biophys. Acta 1852 (2), 209–218.
Xue-Jiao, GUO, Xue-Jiao, FAN, Bin, QIAO, Zhi-Qiang, GE, 2017. A lipophilic prodrug of Danshensu: preparation, characterization, and in vitro and in vivo evaluation. Chinese J. Nat. Med. 15 (5), 355–362.
Yang, Y., Du, L., Zhao, H., Zhao, Y., Liao, S., Zhang, Z., Zhang, S., Bai, Y., Zheng, X., 2025. Danshensu derivatives: A series of promising drugs with protective effects against cardiocerebrovascular diseases and cancers. Med. Res. Rev 45 (4), 1163–1183.
Ye, Y., Xu, W., Zhong, W., Li, Y., Wang, C., 2012. Combination treatment with dihydrotanshinone I and irradiation enhances apoptotic effects in human cervical cancer by HPV E6 down-regulation and caspases activation. Mol. Cell. Biochem 363 (1-2), 191–202.
Yi, X., Wang, F., Feng, Y., Zhu, J., Wu, Y., 2022. Danhong injection attenuates doxorubicin-induced cardiotoxicity in rats via suppression of apoptosis: network pharmacology analysis and experimental validation. Front. Pharmacol 13.
You, J.S., Pan, T.L., Lee, Y.S., 2007. Protective effects of Danshen (Salvia miltiorrhiza) on adriamycin-induced cardiac and hepatic toxicity in rats. Phytother. Res 21 (12), 1146–1152.
Yu, J., Gao, H., Wu, C., Xu, Q.-M., Lu, J.-J., Chen, X., 2018a. Diethyl blechnic, a novel natural product isolated from Salvia miltiorrhiza bunge, inhibits doxorubicin-induced apoptosis by inhibiting ROS and activating JNK1/2. Int. J. Mol. Sci 19 (6).
Yu, J., Wang, C., Kong, Q., Wu, X., Lu, J.J., Chen, X., 2018b. Recent progress in doxorubicin-induced cardiotoxicity and protective potential of natural products. Phytomedicine 40, 125–139.
Yu, L., Qian, J., 2020. Dihydrotanshinone I alleviates spinal cord injury via suppressing inflammatory response, oxidative stress and apoptosis in rats. Med. Sci. Monit 26, e920738.
Yu, M.-l., Li, S.-m., Gao, X., Li, J.-g., Xu, H., Chen, K.-j., 2020. Sodium tanshinone II A sulfonate for coronary heart disease: A systematic review of randomized controlled trials. Chin. J. Integr. Med 26 (3), 219–226.
Yuan, L., Xiao, H., Li, H., Jiang, Y., 2019a. Tanshinone IIA attenuates doxorubicin-induced cardiomyocyte oxidative stress injury through autophagy. Chin. J. Clin. Pharmacol. 35 (19), 2289–2291.
Yuan, R., Huang, L., Du, L.J., Feng, J.F., Li, J., Luo, Y.Y., Xu, Q.M., Yang, S.L., Gao, H., Feng, Y.L., 2019b. Dihydrotanshinone exhibits an anti-inflammatory effect in vitro and in vivo through blocking TLR4 dimerization. Pharmacol. Res 142, 102–114.
Yuan, S.L., Wei, Y.Q., Wang, X.J., Xiao, F., Li, S.F., Zhang, J., 2004. Growth inhibition and apoptosis induction of tanshinone II-A on human hepatocellular carcinoma cells. World. J. Gastroenterol 10 (14), 2024–2028.
Zhang, D.X., Ma, D.Y., Yao, Z.Q., Fu, C.Y., Shi, Y.X., Wang, Q.L., Tang, Q.Q., 2016a. ERK1/2/p53 and NF-κb dependent-PUMA activation involves in doxorubicin-induced cardiomyocyte apoptosis. Eur. Rev. Med. Pharmacol. Sci 20 (11), 2435–2442.
Zhang, J., Li, W., Xue, S., Gao, P., Wang, H., Chen, H., Hong, Y., Sun, Q., Lu, L., Wang, Y., Wang, Q., 2024. Qishen granule attenuates doxorubicin-induced cardiotoxicity by protecting mitochondrial function and reducing oxidative stress through regulation of Sirtuin3. J. Ethnopharmacol 319, 117134.
Zhang, J., Zhang, Q., Liu, G., Zhang, N., 2019. Therapeutic potentials and mechanisms of the Chinese traditional medicine Danshensu. Eur. J. Pharmacol 864, 172710.
Zhang, Q., Liu, J., Duan, H., Li, R., Peng, W., Wu, C., 2021a. Activation of Nrf2/HO-1 signaling: an important molecular mechanism of herbal medicine in the treatment of atherosclerosis via the protection of vascular endothelial cells from oxidative stress. J. Adv. Res 34, 43–63.
Zhang, S., Wei, X., Zhang, H., Wu, Y., Jing, J., Huang, R., Zhou, T., Hu, J., Wu, Y., Li, Y., You, Z., 2023. Doxorubicin downregulates autophagy to promote apoptosis-induced dilated cardiomyopathy via regulating the AMPK/mTOR pathway. Biomed. Pharmacother. 162, 114691.
Zhang, S.H., Su, J., Zhen, Y.S., 2004. [Salvianolic acid A inhibits nucleoside transport and potentiates the antitumor activity of chemotherapeutic drugs]. Yao. Xue. Xue. Bao 39 (7), 496–499.
Zhang, X., Lv, S., Zhang, W., Jia, Q., Wang, L., Ding, Y., Yuan, P., Zhu, Y., Liu, L., Li, Y., Zhang, J., 2021b. Shenmai injection improves doxorubicin cardiotoxicity via miR-30a/Beclin 1. Biomed. Pharmacother 139, 111582.
Zhang, Y., Chen, L., Li, F., Wang, H., Yao, Y., Shu, J., Ying, M.-Z., 2016b. Cryptotanshinone protects against adriamycin-induced mitochondrial dysfunction in cardiomyocytes. Pharm. Biol 54 (2), 237–242.
Zhang, Y., Wei, L., Sun, D., Cao, F., Gao, H., Zhao, L., Du, J., Li, Y., Wang, H., 2010. Tanshinone IIA pretreatment protects myocardium against ischaemia/reperfusion injury through the phosphatidylinositol 3-kinase/akt-dependent pathway in diabetic rats. Diabetes. Obes. Metab. 12 (4), 316–322.

Zhao, R.Z., Jiang, S., Zhang, L., Yu, Z.B., 2019. Mitochondrial electron transport chain, ROS generation and uncoupling (Review). Int. J. Mol. Med 44 (1), 3–15.
Zheng, Z., Ke, L., Ye, S., Shi, P., Yao, H., 2024. Pharmacological mechanisms of cryptotanshinone: recent advances in cardiovascular, Cancer, and neurological disease applications. Drug. Devel. Ther 18, 6031–6060.
Zhong, G.X., Li, P., Zeng, L.J., Guan, J., Li, D.Q., Li, S.P., 2009. Chemical characteristics of salvia miltiorrhiza (Danshen) collected from different locations in China. J. Agric. Food. Chem 57 (15), 6879–6887.
Zhou, G.Y., Jiang, W., Zhao, Y., Ma, G.E., Li, S.G., Xin, W.J., Zhao, B.L., 2002. Interaction between sodium tanshinone IIA sulfonate and the adriamycin semiquinone free radical: A possible mechanism for antagonizing adriamycin-induced cardiotoxity. Res. Chem. Intermed. 28 (4), 277–289.
Zhou, G.Y., Zhao, B.L., Hou, J.W., Ma, G.E., Xin, W.J., 1999. Protective effects of sodium tanshinone IIA sulphonate against adriamycin-induced lipid peroxidation in mice hearts in vivo and in vitro. Pharmacol. Res 40 (6), 487–491.
Zhou, J., Tan, S.-H., Nicolas, V., Bauvy, C., Yang, N.-D., Zhang, J., Xue, Y., Codogno, P., Shen, H.-M., 2013. Activation of lysosomal function in the course of autophagy via mTORC1 suppression and autophagosome-lysosome fusion. Cell. Res 23 (4), 508–523.
Zhou, L., Zuo, Z., Chow, M.S., 2005. Danshen: an overview of its chemistry, pharmacology, pharmacokinetics, and clinical use. J. Clin. Pharmacol 45 (12), 1345–1359.
Zhou, R., He, L.F., Li, Y.J., Shen, Y., Chao, R.B., Du, J.R., 2012. Cardioprotective effect of water and ethanol extract of Salvia miltiorrhiza in an experimental model of myocardial infarction. J. Ethnopharmacol 139 (2), 440–446.
Zhou, W., Yuan, W.F., Chen, C., Wang, S.M., Liang, S.W., 2016. Study on material base and action mechanism of compound Danshen dripping pills for treatment of atherosclerosis based on modularity analysis. J. Ethnopharmacol 193, 36–44.
Zhou, Z.-Y., Zhao, W.-R., Zhang, J., Chen, X.-L., Tang, J.-Y., 2019. Sodium tanshinone IIA sulfonate: a review of pharmacological activity and pharmacokinetics. Biomed. Pharmacother. 118, 109362.
Zou, Y., Lin, L., Ye, Y., Wei, J., Zhou, N., Liang, Y., Gong, H., Li, L., Wu, J., Li, Y., Jia, Z., Wu, Y., Zhou, J., Ge, J., 2012. Qiliqiangxin inhibits the development of cardiac hypertrophy, remodeling, and dysfunction during 4 weeks of pressure overload in mice. J. Cardiovasc. Pharmacol 59 (3), 268–280.
Zraik, I.M., Heß-Busch, Y., 2021. [Management of chemotherapy side effects and their long-term sequelae]. Urol. A 60 (7), 862–871.